

# Towards Lightweight Super-Resolution With Dual Regression Learning

Yong Guo , Mingkui Tan , Zeshuai Deng , Jingdong Wang , Qi Chen, Jiezhang Cao , Yanwu Xu , and Jian Chen

**Abstract**—Deep neural networks have exhibited remarkable performance in image super-resolution (SR) tasks by learning a mapping from low-resolution (LR) images to high-resolution (HR) images. However, the SR problem is typically an ill-posed problem and existing methods would come with several limitations. First, the possible mapping space of SR can be extremely large since there may exist many different HR images that can be super-resolved from the same LR image. As a result, it is hard to directly learn a promising SR mapping from such a large space. Second, it is often inevitable to develop very large models with extremely high computational cost to yield promising SR performance. In practice, one can use model compression techniques to obtain compact models by reducing model redundancy. Nevertheless, it is hard for existing model compression methods to accurately identify the redundant components due to the extremely large SR mapping space. To alleviate the first challenge, we propose a dual regression learning scheme to reduce the space of possible SR mappings. Specifically, in addition to the mapping from LR to HR images, we learn an additional dual regression mapping to estimate the downsampling kernel and reconstruct LR images. In this way, the dual mapping acts as a constraint to reduce the space of possible

mappings. To address the second challenge, we propose a dual regression compression (DRC) method to reduce model redundancy in both layer-level and channel-level based on channel pruning. Specifically, we first develop a channel number search method that minimizes the dual regression loss to determine the redundancy of each layer. Given the searched channel numbers, we further exploit the dual regression manner to evaluate the importance of channels and prune the redundant ones. Extensive experiments show the effectiveness of our method in obtaining accurate and efficient SR models.

**Index Terms**—Image super-resolution, dual regression, closed-loop learning, lightweight models.

## I. INTRODUCTION

DEEP neural networks (DNNs) have been the workhorse of many real-world applications, including image classification [1], [2] and image restoration [3], [4], [5], [6], [7], [8], [9], [10], [11], [12], [13], [14]. Recently, image super-resolution (SR) has become an important task that aims to learn a non-linear mapping to reconstruct high-resolution (HR) images from low-resolution (LR) images. Nevertheless, the SR problem is typically an ill-posed problem and it is non-trivial to learn an effective SR model due to several underlying challenges.

First, the space of possible SR mapping functions can be extremely large since there exist many HR images that can be super-resolved from the same LR image [15]. In practice, most methods directly optimize the reconstruction loss (e.g., MAE or MSE) in HR domain and often easily obtain very blurry results with insufficient high-frequency information [16]. In other words, these undesired blurry solutions may take up the majority of the space of SR mapping to be learned and make the whole learning space extremely large. As a result, it is non-trivial to find a promising one from such a large space. To alleviate this issue, existing methods seek to increase the model capacity (e.g., EDSR [17] and RCAN [18]) and minimize the reconstruction error between the super-resolved images and the ground-truth HR images. However, these methods still suffer from such a large space of possible SR mapping functions (See analysis in Section III-A) and often yield limited performance. Thus, how to reduce the possible space of the mapping functions to boost the training of SR models becomes an important problem.

Second, most SR models often contain a large number of parameters and come with extremely high computational cost. To address this, many efforts have been made to design efficient SR models [19], [20]. However, these models often incur a dramatic performance gap compared with state-of-the-art SR

Manuscript received 23 September 2021; revised 30 December 2023; accepted 11 May 2024. Date of publication 14 June 2024; date of current version 5 November 2024. This work was supported in part by the National Natural Science Foundation of China under Grant 62072190, Grant 62376099, and Grant 62072186, in part by the Key-Area Research and Development Program of Guangdong Province under Grant 2018B010107001, in part by the Program for Guangdong Introducing Innovative and Entrepreneurial Teams under Grant 2017ZT07X183, in part by the Natural Science Foundation of Guangdong Province under Grant 2024A1515010989, and in part by the Major Key Project of PCL under Grant PCL2023A08. Recommended for acceptance by S.J. Kim. (Yong Guo, Mingkui Tan, Zeshuai Deng, and Jian Chen contributed equally to this work.) (Corresponding author: Mingkui Tan.)

Yong Guo and Jian Chen are with the School of Software Engineering, South China University of Technology, Guangzhou 510641, China (e-mail: guoyongcs@gmail.com; ellachen@scut.edu.cn).

Mingkui Tan is with the School of Software Engineering, South China University of Technology, Guangzhou 510641, China, also with Pazhou Laboratory, Guangzhou 510335, China, and also with the Key Laboratory of Big Data and Intelligent Robot (South China University of Technology), Ministry of Education, Guangzhou 510006, China (e-mail: mingkuitan@scut.edu.cn).

Zeshuai Deng is with the School of Software Engineering, South China University of Technology, Guangzhou 510641, China, and also with Pengcheng Laboratory, Shenzhen 518066, China (e-mail: sedengzeshuai@mail.scut.edu.cn).

Jingdong Wang is with Baidu Inc., Beijing 100080, China (e-mail: wangjingdong@baidu.com).

Qi Chen is with the Faculty of Engineering, The University of Adelaide, Adelaide, SA 5005, Australia (e-mail: qi.chen04@adelaide.edu.au).

Jiezhang Cao is with ETH Zürich, 8092 Zürich, Switzerland (e-mail: jiezhang.cao@vision.ee.ethz.ch).

Yanwu Xu is with the School of Future Technology, South China University of Technology, Guangzhou 510641, China (e-mail: ywxu@ieee.org).

This article has supplementary downloadable material available at <https://doi.org/10.1109/TPAMI.2024.3406556>, provided by the authors.

Digital Object Identifier 10.1109/TPAMI.2024.3406556

TABLE I  
PERFORMANCE COMPARISONS FOR 4 $\times$  IMAGE SUPER-RESOLUTION

Method	#Params (M)	#Madds (G)	Set5 PSNR / SSIM	Set14 PSNR / SSIM	BSDS100 PSNR / SSIM	Urban100 PSNR / SSIM	Manga109 PSNR / SSIM
Bicubic	-	-	28.42 / 0.810	26.10 / 0.702	25.96 / 0.667	23.15 / 0.657	24.92 / 0.789
ESPCN [94]	-	0.2	29.21 / 0.851	26.40 / 0.744	25.50 / 0.696	24.02 / 0.726	23.55 / 0.795
LapSRN [95]	0.9	29.2	31.54 / 0.885	28.09 / 0.770	27.31 / 0.727	25.21 / 0.756	29.09 / 0.890
DRRN [96]	0.3	1087.5	31.68 / 0.889	28.21 / 0.772	27.38 / 0.728	25.44 / 0.764	29.46 / 0.896
CARN [97]	1.1	14.6	32.13 / 0.894	28.60 / 0.781	27.58 / 0.735	26.07 / 0.784	30.47 / 0.908
IMDN [98]	0.7	6.6	32.21 / 0.895	28.58 / 0.781	27.56 / 0.735	26.04 / 0.784	30.45 / 0.908
PAN [99]	0.3	4.5	32.13 / 0.895	28.61 / 0.782	27.59 / 0.736	26.11 / 0.785	30.51 / 0.910
SRResNet [32]	1.5	20.5	32.05 / 0.891	28.49 / 0.782	27.61 / 0.736	26.09 / 0.783	30.70 / 0.908
SRGAN [32]	1.5	20.5	29.46 / 0.838	26.60 / 0.718	25.74 / 0.666	24.50 / 0.736	27.79 / 0.856
ECBSR [49]	0.6	5.5	31.92 / 0.895	28.34 / 0.782	27.48 / 0.739	25.81 / 0.777	-
SMSR [53]	1.0	-	32.12 / 0.893	28.55 / 0.781	27.55 / 0.735	26.11 / 0.787	30.54 / 0.909
SR-APS [55]	0.1	-	31.93 / 0.891	28.42 / 0.776	27.44 / 0.731	25.66 / 0.772	-
DFSR [52]	10.8	116.1	31.78 / 0.890	28.33 / 0.7758	27.38 / 0.729	25.40 / 0.761	-
SRDenseNet [33]	2.0	62.3	32.02 / 0.893	28.50 / 0.778	27.53 / 0.733	26.05 / 0.781	29.49 / 0.899
EDSR [17]	43.1	463.1	32.48 / 0.898	28.81 / 0.787	27.72 / 0.742	26.64 / 0.803	31.03 / 0.915
DBPN [28]	15.3	1220.4	32.42 / 0.897	28.75 / 0.786	27.67 / 0.739	26.38 / 0.794	30.90 / 0.913
RCAN [18]	15.6	147.1	32.63 / 0.900	28.85 / 0.788	27.74 / 0.743	26.74 / 0.806	31.19 / 0.917
RRDB [100]	16.7	165.2	32.73 / 0.901	28.97 / 0.790	27.83 / 0.745	27.02 / 0.815	31.64 / 0.919
HAN [22]	16.2	151.5	32.61 / 0.900	28.90 / 0.789	27.79 / 0.744	26.85 / 0.809	31.44 / 0.918
CSNLN [21]	6.6	4428.5	32.68 / 0.900	28.95 / 0.789	27.80 / 0.744	27.22 / 0.817	31.43 / 0.920
SAN [101]	15.8	150.1	32.64 / 0.900	28.92 / 0.788	27.79 / 0.743	26.79 / 0.806	31.18 / 0.916
ClassSR [12]	30.1	-	32.25 / 0.898	28.77 / 0.788	27.65 / 0.741	26.70 / 0.804	31.17 / 0.916
SwinIR [44]	11.9	121.1	32.92 / 0.904	29.09 / 0.795	27.92 / 0.749	27.45 / 0.825	32.05 / 0.926
DAT [45]	14.8	155.1	33.08 / 0.906	29.23 / 0.797	28.00 / 0.751	27.87 / 0.834	32.51 / 0.929
DRN-S	4.8	109.9	32.68 / 0.901	28.93 / 0.790	27.78 / 0.744	26.84 / 0.807	31.52 / 0.919
DRN-L	9.8	224.8	32.74 / 0.902	28.98 / 0.792	27.83 / 0.745	27.03 / 0.813	31.73 / 0.922
SwinIR-DR	11.9	121.1	33.03 / 0.904	29.19 / 0.795	27.98 / 0.747	27.80 / 0.831	32.38 / 0.925
DAT-DR	14.8	155.1	33.17 / 0.906	29.30 / 0.798	28.04 / 0.752	28.04 / 0.837	32.71 / 0.930

"-" denotes the results that are not reported. We highlight that our dual regression (DR) method is able to enhance both CNN-based and transformer-based SR models, showing a high flexibility on top of diverse architectures.

methods [21], [22]. Unlike these methods, one can also exploit model compression techniques (e.g., channel pruning) to obtain lightweight models. Nevertheless, it is non-trivial to identify the redundant components (e.g., channels) in SR models due to the large possible mapping space. Specifically, given an inaccurate SR mapping, the estimated/predicted redundancy of model components may be also very inaccurate. More critically, the redundancy may vary a lot among different layers in the model and different channels in each layer, making it harder to identify the redundant components.

In this paper, we propose a novel dual regression learning scheme to obtain accurate and efficient SR models. To reduce the possible mapping space, we introduce an additional constraint that encourages the super-resolved images to reconstruct the input LR images. Suppose there are some high-frequency textures (e.g., contour of object or human hair) inside LR images, this constraint guarantees that the super-resolved images are able to preserve the high-frequency information if they can perfectly reconstruct the original LR images. In other words, we are able to effectively exclude a large number of solutions that catastrophically lose these high-frequency textures even though they perform very well on the low-frequency parts (often with a very small loss w.r.t. MAE or MSE). With this constraint, the dual regression scheme improves SR performance by reducing the space of possible SR mappings, yielding a smaller generalization bound than existing methods (See Theorem 1).

To obtain effective lightweight SR models, we propose a search-guided pruning pipeline, named the dual regression

compression (DRC) method, to reduce the model redundancy in both layer-level and channel-level. Specifically, we first determine the redundancy of each layer by performing channel number search with our dual regression scheme. Unlike existing methods, we design an importance-aware search strategy to facilitate the channel number search for pruning. Then, we exploit the dual regression scheme to evaluate the importance of channels and prune those redundant ones according to the searched channel numbers. Extensive experiments under both the non-blind and blind SR settings demonstrate the superiority of our method (See results in Tables I, II and III).

Our contributions are summarized as follows:

- To alleviate the issue of extremely large SR mapping space incurred by the nature of ill-posed problems, we propose a dual regression learning scheme that introduces an additional dual mapping to reconstruct LR images. The dual mapping acts as a constraint to reduce the space of possible SR mapping functions and enhance the training of SR models.
- Unlike most model compression methods, we propose a search-guided pruning pipeline, dual regression compression method (DRC), to exploit a reduced mapping space to identify both the layer-level and channel-level redundancy. Specifically, we design an importance-aware search strategy to identify the redundancy of each layer and search for a promising channel configuration for the subsequent pruning process. Then, we conduct channel pruning to remove the redundant

TABLE II  
COMPARISON WITH LIGHTWEIGHT SR MODELS AND PRUNING METHODS ON FIVE BENCHMARKS FOR 4× SR

Model	Method	#Params (K)	#Madds (G)	Set5 PSNR / SSIM	Set14 PSNR / SSIM	BSDS100 PSNR / SSIM	Urban100 PSNR / SSIM	Manga109 PSNR / SSIM
SRCCNN [117]		57	8.5	30.48 / 0.863	27.49 / 0.750	26.90 / 0.710	24.52 / 0.722	27.66 / 0.851
FSRCCNN [19]		12	0.7	30.71 / 0.866	27.59 / 0.754	26.98 / 0.710	24.62 / 0.728	27.90 / 0.852
CARN-M [97]		300	5.2	31.92 / 0.890	28.42 / 0.776	27.44 / 0.730	25.62 / 0.769	25.62 / 0.769
VDSR [39]		665	612.6	31.35 / 0.883	28.01 / 0.767	27.29 / 0.725	25.18 / 0.752	-
LapSRN [95]		813	149.4	31.54 / 0.885	28.19 / 0.777	27.32 / 0.728	25.21 / 0.756	-
DRRN [96]		297	6,796.9	31.68 / 0.888	28.21 / 0.772	27.38 / 0.728	25.44 / 0.763	-
MemNet [117]		677	2,662.4	31.74 / 0.889	28.26 / 0.772	27.40 / 0.728	25.50 / 0.763	-
IMDN [98]		715	40.9	32.21 / 0.894	28.58 / 0.781	27.56 / 0.735	26.04 / 0.783	30.45 / 0.907
LAPAR-A [118]		659	94.0	32.15 / 0.894	28.61 / 0.781	27.61 / 0.736	26.14 / 0.787	30.42 / 0.907
LatticeNet [119]		777	43.6	32.30 / 0.896	28.68 / 0.783	27.62 / 0.736	26.25 / 0.787	-
DI-trim-0.3-SRResNet [70]		604	14.9	32.32 / 0.894	28.70 / 0.783	27.60 / 0.737	26.14 / 0.786	-
SMSR [53]		1006	-	32.12 / 0.893	28.55 / 0.781	27.55 / 0.735	26.11 / 0.787	30.54 / 0.909
NAPS [55]		125	7.1	31.93 / 0.867	27.68 / 0.756	26.98 / 0.716	24.65 / 0.730	-
SRPN-Lite [73]		623	35.8	32.24 / 0.896	28.69 / 0.784	27.63 / 0.737	26.16 / 0.788	-
ELAN-light [120]		640	53.72	32.43 / 0.897	28.78 / 0.785	27.69 / 0.740	26.54 / 0.798	30.92 / 0.915
DRN-S		Baseline	4800	109.9	32.68 / 0.901	28.93 / 0.790	27.78 / 0.744	26.84 / 0.807
DRN-S	CP [121]	3473	77.4	32.26 / 0.887	28.47 / 0.777	27.38 / 0.732	26.42 / 0.794	31.03 / 0.904
	ThiNet [58]	3473	77.4	32.33 / 0.889	28.57 / 0.781	27.45 / 0.734	26.53 / 0.796	31.12 / 0.907
	DCP [60]	3473	77.4	32.41 / 0.893	28.65 / 0.782	27.52 / 0.737	26.61 / 0.800	31.21 / 0.912
	SRP [73]	3473	77.4	32.49 / 0.894	28.77 / 0.786	27.63 / 0.740	26.80 / 0.806	31.44 / 0.917
	DRC (Ours)	3116	72.3	<b>32.66 / 0.900</b>	<b>28.92 / 0.789</b>	<b>27.82 / 0.744</b>	<b>26.95 / 0.809</b>	<b>31.64 / 0.921</b>
SwinIR-light [44]		Baseline	897	10.0	32.44 / 0.897	28.77 / 0.785	27.69 / 0.740	26.47 / 0.798
SwinIR-light [44]	CP [121]	689	7.3	32.05 / 0.883	28.34 / 0.771	27.36 / 0.730	26.13 / 0.789	30.57 / 0.910
	ThiNet [58]	689	7.3	32.24 / 0.888	28.57 / 0.775	27.42 / 0.732	26.25 / 0.791	30.74 / 0.912
	DCP [60]	689	7.3	32.27 / 0.891	28.66 / 0.780	27.52 / 0.735	26.31 / 0.793	30.79 / 0.911
	SRP [73]	689	7.3	30.31 / 0.892	28.71 / 0.781	27.51 / 0.735	26.33 / 0.794	30.82 / 0.913
	DRC (Ours)	635	6.8	<b>32.44 / 0.896</b>	<b>28.81 / 0.785</b>	<b>27.70 / 0.738</b>	<b>26.44 / 0.797</b>	<b>30.94 / 0.915</b>

We consider the pruning ratio of 30% for all the pruning methods for fair comparison. We highlight that our pruned model consistently outperforms all the considered lightweight SR models as well as the pruning methods.

TABLE III  
QUANTITATIVE COMPARISONS ON DIV2KRK [113] UNDER THE BLIND SETTING. ON.

Method	#Params (M)	#Madds (G)	PSNR	SSIM
Bicubic	-	-	25.33	0.679
Bicubic+ZSSR [30]	0.2	-	25.61	0.691
EDSR [17]	43.1	463.1	25.64	0.692
RCAN [18]	15.6	147.1	25.66	0.693
DBPN [28]	15.3	1220.4	25.58	0.691
DBPN [28]+Correction [122]	10.4	-	26.79	0.742
KernelGAN [112]+SRMD [41]	1.7	-	27.51	0.726
KernelGAN [112]+ZSSR [30]	0.4	-	26.81	0.731
IKC [31]	5.3	404.5	27.70	0.766
DANv1 [123]	4.3	175.8	27.55	0.758
DANv2 [124]	4.7	174.1	28.74	0.789
AdaTarget [125]	16.7	165.2	28.44	0.787
KOALAnet [126]	6.5	64.3	27.77	0.763
FKP [13]+USRNet [127]	0.7	-	21.56	0.606
BSRDM [128]	0.8	-	23.08	0.632
Real-RRDB(p=0.5) [129]	16.7	165.2	28.53	0.790
DCLS [116]	19.1	69.9	28.99	0.795
DCLS-DRC (Ours)	14.2	57.1	29.01	0.798

“-” denotes the results that are not reported or not applicable. We highlight that, taking DCLS [117] as the baseline, our DRC achieves lossless compression while greatly reducing the number of parameters.

channels according to the searched channel number configuration.

- Extensive experiments demonstrate the flexibility of our dual regression scheme for SR. In practice, our method is applicable to boost the training and model compression for both CNN-based and transformer-based SR models. Furthermore, we demonstrate that our DRC scheme is able to achieve a lossless compression to reduce the computational cost under both the non-blind and the blind SR settings.

This paper extends our preliminary version [23] from several aspects. 1) We propose a dual regression compression scheme

(DRC) to achieve lossless compression for SR models. Unlike most existing methods, our DRC simultaneously conduct channel number search and channel pruning to enhance the performance of model compression. 2) We present a dual regression based channel number search method to identify the layer-level redundancy by determining the number of channels for each layer. During the search process, we design an importance-aware search strategy to facilitate the channel number search for pruning. 3) We develop a dual regression based channel pruning algorithm that exploits the dual regression manner to evaluate the importance of channels when performing channel pruning. 4) We conduct more experiments on both CNN-based and transformer-based SR models to investigate the effect of our dual regression scheme. 5) We demonstrate the effectiveness of our dual regression compression scheme under both the non-blind and blind SR settings.

## II. RELATED WORK

### A. Image Super-Resolution

Existing SR methods mainly include interpolation-based approaches [24], [25], [26], [27] and reconstruction-based methods [18], [28], [29], [30], [31]. Interpolation-based methods may oversimplify the SR problem and usually generate blurry images [32], [33]. The reconstruction-based methods [34], [35], [36] reconstruct the HR images from LR images. Following such methods, many CNN-based methods [37], [38], [39], [40], [41], [42], [43] were developed to learn a reconstruction mapping.

Recently, Ledig et al. [32] propose a deep residual network SRResNet for super-resolution. Lim et al. [17] remove unnecessary modules in the residual network [1] and design a very wide network EDSR. Haris et al. [28] propose a back-projection

network (DBPN) to iteratively produce LR and HR images. Zhang et al. [18] propose a channel attention mechanism to build a deep model called RCAN to further improve the SR performance. Mei et al. [21] propose a Cross-Scale Non-Local attention module for more accurate image SR. Niu et al. [22] propose a holistic attention network (HAN) to model the interdependencies among layers, channels, and spatial positions. Liang et al. [44] develop a transformer model to improve the performance of image restoration. Chen et al. [45] further propose a dual aggregation transformer to effectively aggregate features across spatial and channel dimensions. Moreover, Zhang et al. [46] focus on blind deblurring and develop a pixel screening based intermediate correction method. However, the training process of these methods still has a very large space of the possible SR mappings, making it hard to learn a good solution in practice.

### B. Lightweight Model Techniques

Lightweight models have gained great attention in recent years [47], [48]. One can obtain lightweight models by directly designing efficient architectures or distilling knowledge from other models. Hui et al. [20] propose an information distillation block to extract the local long and short-path features for lightweight SR networks. Zhang et al. [49] propose a re-parameterizable building block for efficient SR. However, these models often incur a dramatic performance gap compared to state-of-the-art SR methods [21], [22]. Besides these methods, one can enhance the lightweight SR performance using knowledge distillation technique [50], [51], [52]. Gao et al. [50] use a lightweight student SR model to learn the knowledge from the deeper teacher SR network. Lee et al. [51] propose a distillation framework that leverages HR images as privileged information to boost the training of the student network. Wang et al. [53] explore the sparsity in image SR and predict a pixel-level redundancy mask to improve the inference efficiency of SR networks. Yu et al. [51] propose a hyperparameter optimization method to search for an efficient architecture for super-resolution from scratch. Yu et al. [54] shares a similar idea with us to search/find the optimal number of channels. However, both methods define a very limited search space where all the blocks/cells share the same number of channels, ignoring the differences of redundancy among different layers. Thus, they cannot identify the layer-wise redundancy of channels and may still result in suboptimal model performance. Zhan et al. [55] further combine neural architecture search with layer-wise pruning strategy to obtain efficient SR models.

Besides these methods, we can also use model compression techniques to obtain lightweight models [56], [57], [58], [59]. As one of the predominant approaches, channel pruning [60], [61], [62], [63], [64], [65] seeks to remove the redundant channels of deep models to obtain compact subnets. It has been shown that these subnets often come with promising accuracy [66] and robustness [67], [68], [69]. Recently, Hou et al. [70] use conditional covariance [71] to measure the importance of channels to the final output of SR models. Li et al. [72] propose a differentiable meta channel pruning method (DHP) to compress

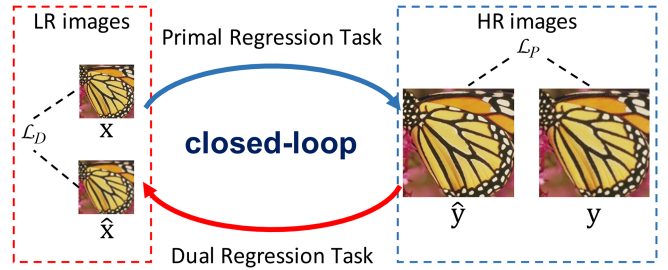


Fig. 1. The proposed dual regression learning scheme contains a primal regression task for SR and a dual regression task to reconstruct LR images. The primal and dual regression tasks form a closed-loop.

SR models. Zhang et al. [73] impose regularization on the pruned structure to ensure the locations of pruned filters are aligned across different layers of residual blocks. In addition, some quantization-based methods [74], [75], [76] exploit low bits to accelerate the inference speed of SR models. However, it is still non-trivial for these methods to identify the redundant components due to the extremely large possible function space.

Unlike them, we seek to reduce the possible function space to alleviate the training/compression difficulty. Thus, it becomes possible to obtain lightweight SR models without significant performance degradation (See Table II).

### C. Dual Learning

Dual learning [77], [78], [79], [80] contains a primal model and a dual model and learns two opposite mappings simultaneously to enhance the performance of language translation. Recently, this scheme has also been used to perform image translation without paired training data [81], [82]. Specifically, a cycle consistency loss is proposed to avoid the mode collapse issue of GAN methods [81], [83], [84] and help minimize the distribution divergence. However, these methods cannot be directly applied to the standard SR problem. By contrast, we use the closed-loop to reduce the space of possible functions of SR. Moreover, we consider learning asymmetric mappings and provide a theoretical guarantee on the rationality and necessity of using a cycle.

## III. DUAL REGRESSION NETWORKS

In this paper, we propose a dual regression learning scheme to obtain accurate and efficient SR models. As shown in Fig. 1, we introduce a constraint on LR images to reduce the space of possible SR mapping functions. To further reduce the model redundancy, we propose a dual regression compression (DRC) method to compress large models (See Fig. 2). For convenience, we term our models Dual Regression Networks (DRNs).

### A. Dual Regression Learning for Super-Resolution

Due to the nature of the ill-posed problems, the space of possible SR mapping functions can be extremely large, making the training very difficult. To alleviate this issue, we propose a dual regression learning scheme by introducing an additional constraint on LR data. From Fig. 1, besides the mapping  $\text{LR} \rightarrow \text{HR}$ ,

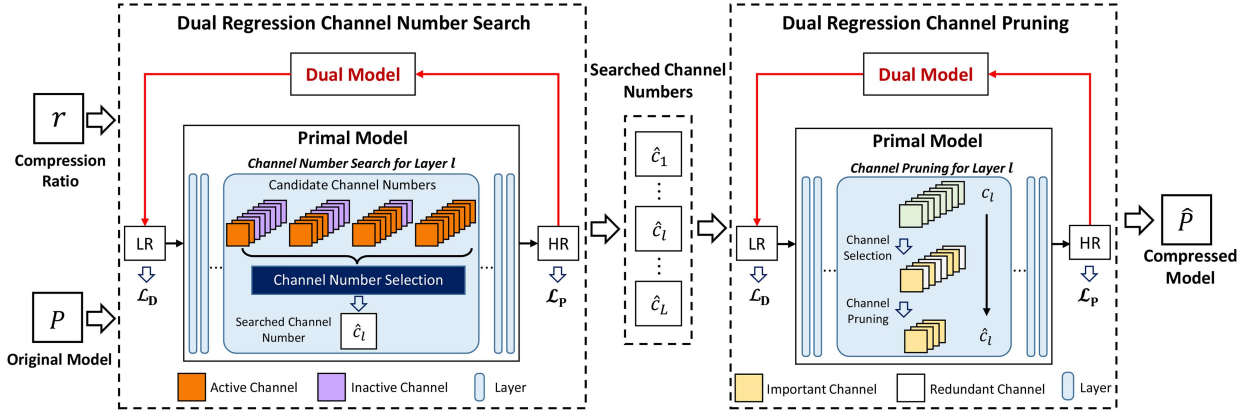


Fig. 2. Overview of the *dual regression compression (DRC)* approach. Given a target compression ratio  $r$ , we first determine the redundancy of each layer by performing the dual regression based channel number search. Then, according to the searched channel numbers, we evaluate the importance of channels and prune those redundant ones to obtain the compressed model  $\hat{P}$ .

we also learn an inverse/dual mapping from the super-resolved images back to LR images. Let  $\mathbf{x} \in \mathcal{X}$  be LR images and  $\mathbf{y} \in \mathcal{Y}$  be HR images. Unlike existing methods, we simultaneously learn a primal mapping  $P$  to reconstruct HR images and a dual mapping  $D$  to reconstruct LR images. Formally, we formulate the SR problem into the dual regression learning scheme which involves two regression tasks.

**Definition 1 (Primal Regression Task for SR):** We seek to find a function  $P: \mathcal{X} \rightarrow \mathcal{Y}$ , such that the prediction  $P(\mathbf{x})$  is similar to its corresponding HR image  $\mathbf{y}$ .

**Definition 2 (Dual Regression Task for SR):** We seek to find a function  $D: \mathcal{Y} \rightarrow \mathcal{X}$ , such that the prediction of  $D(\mathbf{y})$  is similar to the original input LR image  $\mathbf{x}$ .

The primal and dual learning tasks form a closed-loop and provide important supervision to train the models  $P$  and  $D$ . If  $P(\mathbf{x})$  was the correct HR image, then the downsampled image  $D(P(\mathbf{x}))$  should be very close to the input LR image  $\mathbf{x}$ . By jointly learning these two tasks, we train the models based on  $N$  paired samples  $\{(\mathbf{x}_i, \mathbf{y}_i)\}_{i=1}^N$ , where  $\mathbf{x}_i$  and  $\mathbf{y}_i$  denote the  $i$ th pair of LR and HR images. Let  $\mathcal{L}_P$  and  $\mathcal{L}_D$  be the loss function ( $\ell_1$ -norm) for the primal and dual tasks, respectively. The training loss becomes

$$\begin{aligned} \mathcal{L}_{\text{DR}}(P, D) = & \frac{1}{N} \sum_{i=1}^N \underbrace{\mathcal{L}_P(P(\mathbf{x}_i), \mathbf{y}_i)}_{\text{primal regression loss}} \\ & + \lambda \underbrace{\mathcal{L}_D(D(P(\mathbf{x}_i)), \mathbf{x}_i)}_{\text{dual regression loss}}. \end{aligned} \quad (1)$$

Here,  $\lambda$  controls the weight of the dual regression loss (See the sensitivity analysis of  $\lambda$  in Section V-D).

More critically, we also theoretically justify our method. In practice, our method has a smaller generalization bound than the vanilla training methods (i.e., without the dual mapping). In other words, our method helps to learn a more accurate  $\mathbf{LR} \rightarrow \mathbf{HR}$  mapping and improve SR performance. We summarize the theoretical analysis in Theorem 1 and put the proof in supplementary.

**Theorem 1:** Let  $\mathcal{L}_{\text{DR}}(P, D)$  be a mapping from  $\mathcal{X} \times \mathcal{Y}$  to  $[0, 1]$  and  $\mathcal{H}_{\text{dual}}$  be the function space. Let  $N$  denote the number of samples and  $\hat{R}_{\mathcal{Z}}^{DL}$  represent the empirical Rademacher complexity [85] of dual learning. We use  $\mathcal{B}(P), P \in \mathcal{H}$  to denote the generalization bound of the supervised learning w.r.t. the Rademacher complexity  $\hat{R}_{\mathcal{Z}}^{SL}(\mathcal{H})$ . For any error  $\delta > 0$ , the generalization bound of the dual regression scheme is  $\mathcal{B}(P, D) = 2\hat{R}_{\mathcal{Z}}^{DL}(\mathcal{H}_{\text{dual}}) + 3\sqrt{\frac{1}{2N} \log(\frac{2}{\delta})}$ . Based on the definition of the Rademacher complexity, the capacity of the function space  $\mathcal{H}_{\text{dual}}$  is smaller than the capacity of function space  $\mathcal{H}$ , i.e.,  $\hat{R}_{\mathcal{Z}}^{DL} \leq \hat{R}_{\mathcal{Z}}^{SL}$ . In this sense, the dual regression scheme has a smaller generalization bound than the vanilla learning scheme

$$\mathcal{B}(P, D) \leq \mathcal{B}(P).$$

**Differences from CycleGAN based methods [81], [82]:** Both DRN and CycleGAN [81] exploit the similar idea of building a cycle, but they have several essential differences. *First*, they consider different objectives. CycleGAN uses cycles to help minimize distribution divergence but DRN builds a cycle to improve reconstruction performance. *Second*, they consider different cycle/dual mappings. CycleGAN learns two symmetric mappings but DRN considers learning asymmetric mappings. Essentially, the primal mapping  $\mathbf{LR} \rightarrow \mathbf{HR}$  is much more complex than the dual mapping  $\mathbf{HR} \rightarrow \mathbf{LR}$ . Considering this, we design the dual model with a very small CNN (See the detailed model design in supplementary) and introduce a tradeoff parameter  $\lambda$  in (1). *Third*, our dual regression method is a more general scheme that can be used in more application scenarios than CycleGAN. Specifically, our method is a plug-and-play module that can be used to enhance diverse SR models and/or conduct model compression. By contrast, CycleGAN cannot be directly applied on top of diverse SR models since it naturally requires the dual model to have the same architecture as the original/primal model. Such a large dual model may increase the training difficulty and introduce a lot of redundancy. Instead, our method builds a very simple dual model that is more suitable for SR tasks where the downsampling mapping is much easier to learn than the upsampling mapping. Experiments show that

**Algorithm 1:** Dual Regression Based Channel Number Search.

---

**Input:** Training data  $\mathcal{S}^{\text{train}}$  and validation data  $\mathcal{S}^{\text{val}}$ ;  
Original channel numbers  $\{c_l\}_{l=1}^L$ ;  
Channel number configurations  $\{\alpha_l\}_{l=1}^L$ ;  
Candidate scaling factors  $\mathcal{V}$ ;  
Target compression ratio  $r$ .

**Output:** Searched channel numbers  $\{\hat{c}_l\}_{l=1}^L$ .

- 1 Rebuild model  $\alpha$  with configuration parameters  $\{\alpha_l\}_{l=1}^L$ ;
- 2 **while** not converge **do**
- 3   // Update the channel number configuration  $\alpha$
- 4   Sample data batch from  $\mathcal{S}^{\text{val}}$  to compute  $\mathcal{L}_{\text{DR}}^{\text{val}}$ ;
- 5   Evaluate channel importance and rank the channels;
- 6   Update  $\alpha$  by descending  $\nabla_{\alpha} \mathcal{L}_{\text{DR}}^{\text{val}}((\alpha; \mathbf{W}^*), D)$ ;
- 7   // Update model parameters  $\mathbf{W}$
- 8   Sample data batch from  $\mathcal{S}^{\text{train}}$  to compute  $\mathcal{L}_{\text{DR}}^{\text{train}}$ ;
- 9   Update  $\mathbf{W}$  by descending  $\nabla_{\mathbf{W}} \mathcal{L}_{\text{DR}}^{\text{train}}((\alpha; \mathbf{W}), D)$ ;
- 10 **end**
- 11 **for**  $l = 1$  to  $L$  **do**
- 12   Select the scaling factor  $\hat{v} = \arg \max_{v \in \mathcal{V}} \alpha_l^{(v)}$ ;
- 13   Compute the channel number  $\hat{c}_l = c_l \cdot (1 - r) \cdot \hat{v}$ ;
- 14 **end**

---

DRC performs well on both CNN-based and transformer-based architectures, and under both non-blind and blind SR settings (See results in Tables I, II, and III).

### B. Dual Regression Compression

Most SR models have extremely high computational cost and cannot be directly deployed to the devices with limited computation resources. To alleviate this issue, one can apply model compression techniques to obtain lightweight models. However, it is non-trivial to accurately identify the redundant components (e.g., layers or channels) due to the extremely large mapping space. Specifically, once we learn an inaccurate SR mapping, the predicted model redundancy may be also inaccurate, leading to significant performance drop (See results in Tables II).

To address the above issues, we build a lightweight dual regression compression method based on channel pruning techniques to compress SR models in a reduced mapping space. Let  $\psi(\cdot)$  be the function to measure the computational cost of models (e.g., the number of parameters). Given a primal model  $P$  and a target compression ratio  $r$ , we seek to obtain a compressed model  $\widehat{P}$  that satisfies the constraint  $\psi(\widehat{P}) \leq (1 - r)\psi(P)$ . Supposing that both  $P$  and  $\widehat{P}$  share the same dual model  $D$ , the optimization problem becomes

$$\min_{\widehat{P}} \mathcal{L}_{\text{DR}}(\widehat{P}, D) \quad \text{s.t. } \psi(\widehat{P}) \leq (1 - r)\psi(P). \quad (2)$$

In this paper, we seek to reduce the model redundancy in both layer-level and channel-level. As shown in Fig. 2, we first determine the redundancy for each layer by performing dual regression channel number search. Then, we exploit the dual regression scheme to evaluate the importance of channels and prune the redundant ones according to the searched channel numbers.

**1) Dual Regression Based Channel Number Search:** Most channel pruning methods adopt a hand-crafted compression policy to prune deep models [90], [91], e.g., pruning 50% channels in all the layers. However, such a compression policy may not be optimal since different layers often have different redundancy [92]. To address this issue, we propose a dual regression channel number search method to recognize the redundancy of each layer by determining the promising number of channels to be preserved. To save the training cost, we follow [65], [89] and use the weight-sharing strategy. Unlike existing search methods, we propose an importance-aware search strategy to select channels according to their importance during the search process. We show the details of the proposed method in Algorithm 1.

Given a primal model  $P$  with  $L$  layers, we use  $\{c_l\}_{l=1}^L$  to denote the channel numbers of different layers. To obtain a model that satisfies the target compression ratio  $r$ , for any layer  $l$ , we first remove  $c_l \cdot r$  channels and then investigate whether we can further remove more channels without degrading the performance. Nevertheless, the search space would be extremely large since the candidate channel number can be any positive integer lower than  $c_l$ . To alleviate this issue, we construct the search space by considering a set of candidate scaling factors  $\mathcal{V} = \{50\%, 60\%, 70\%, 80\%, 90\%, 100\%\}$  to scale the channel number. Specifically, for the  $l$ th layer, we seek to select a scaling factor  $\hat{v} \in \mathcal{V}$  to obtain the resultant channel number  $\hat{c}_l = c_l \cdot (1 - r) \cdot \hat{v}$  in the compressed model. Notably, for the  $l$ th layer, we use  $r$  to define the maximum number of channels  $c_l \cdot (1 - r)$ , which acts as the upper bound of the candidate channel numbers during the search process. We use six  $v$  for each layer to define the search space of candidate channel numbers, which enables selecting different channel numbers that are not larger than the upper bound.

Given a target compression ratio  $r$  and a candidate scaling factor  $v$ , we need to select  $k = c_l \cdot (1 - r) \cdot v$  channels to build the  $l$ th layer. As shown in Fig. 4(a) and (b), most search methods do not consider the importance of channels when determining the optimal channel configuration. The ignorance of channel importance may cause inconsistency between channel number search and channel pruning, resulting in limited performance (See Table IV). To address this issue, we adopt the consistent criterion of evaluating channel importance during both the search process and the following pruning process. As shown in Fig. 4(c), we first rank the channels according to their importance in terms of the  $\ell_1$ -norm on the weights of each channel. Then, we selected the top- $k$  important channels based on the ranking result. In this sense, we optimize the top- $k$  important channels instead of only the first  $k$  channels. We highlight that the importance rank of channels can be continuously updated during the search process since we also optimize the weights at the same time.

To find the promising channel configurations, we adopt the differentiable search strategy [93] by relaxing the search space to be continuous. For any layer  $l$ , we construct a channel number configuration  $\alpha_l \in \mathbb{R}^{|\mathcal{V}|}$  in which each element  $\alpha_l^{(v)}$  indicates the importance of a specific scaling factor  $v$ . For any layer  $l$ , let  $\mathbf{X}^{(l)}$  be the input features,  $\mathbf{W}^{(l)}$  be the parameters, and  $\otimes$

TABLE IV  
EFFECT OF IMPORTANCE-AWARE SEARCH AND DUAL REGRESSION SCHEME ON SR MODEL COMPRESSION FOR  $4 \times$  SR

Method	Channel-wise Weight Sharing	Importance-aware Search	Dual	Search Cost (h)	#Params (M)	MAdds (G)	PSNR on Set5
Manually Designed Random Search	-	-	-	-	3.4	77.4	32.33
DARTS [93]	✗ ✓	✗ ✗	✗ ✗	23 10	3.2 3.3	73.9 75.0	32.27 32.40
DRC	✓ ✓	✓ ✓	✗ ✓	10 10	3.2 3.1	74.6 72.3	32.53 <b>32.66</b>

Interestingly, we find that weight sharing is able to greatly reduce the search cost while obtaining similar search results with the baseline DARTS approach. More critically, when comparing the fifth and the sixth rows, the importance-aware search strategy is particularly effective in finding a smaller model but with better performance. If we further apply our dual regression scheme, we obtain the best result among the considered variants.

be the convolutional operation. For convenience, we use  $\mathbf{X}_{[1:k]}^{(l)}$  and  $\mathbf{W}_{[1:k]}^{(l)}$  to denote the features and parameters w.r.t. the top- $k$  important channels (see the channel selection in Fig. 4(c)). In this paper, we use  $c_l^{(v)}$  to denote the number of channels specified by a specific scaling factor  $v$ . Following [93], we relax the categorical choice of a particular factor as a softmax over all possible factors. Then, we use the sum operation to make the search space continuous and the search process differentiable. Formally, the output of the  $l$ th layer is

$$\mathbf{X}^{(l+1)} = \sum_{v \in \mathcal{V}} \frac{\exp(\alpha_l^{(v)})}{\sum_{v' \in \mathcal{V}} \exp(\alpha_l^{(v')})} \mathbf{X}_{[1:c_l^{(v)}]}^{(l)} \otimes \mathbf{W}_{[1:c_l^{(v)}]}^{(l)}. \quad (3)$$

With the continuous relaxation, the task of channel number search becomes learning a set of continuous variables  $\boldsymbol{\alpha} = \{\alpha_l\}_{l=1}^L$ . As shown in Algorithm 1, for any layer  $l$ , we obtain the resultant channel numbers by selecting the most likely element in  $\alpha_l$ .

Due to the extremely large function space of the ill-posed SR problem that contains a lot of undesired blurry solutions, it is non-trivial to accurately identify the redundancy of each layer for most search methods. To enhance the search process, we minimize the dual regression loss to reduce the space of possible mapping functions. Let  $\mathcal{L}_{\text{DR}}^{\text{train}}$  and  $\mathcal{L}_{\text{DR}}^{\text{val}}$  be the dual regression loss computed on the training data and validation data. Here, we use the continuous variables  $\boldsymbol{\alpha}$  and the model parameters  $\mathbf{W}$  to represent the primal model  $P = (\boldsymbol{\alpha}; \mathbf{W})$ . Given a dual model  $D$ , the optimization problem of channel number search becomes

$$\begin{aligned} & \min_{\boldsymbol{\alpha}} \mathcal{L}_{\text{DR}}^{\text{val}}((\boldsymbol{\alpha}; \mathbf{W}^*), D) \\ & \text{s.t. } \mathbf{W}^* = \operatorname{argmin}_{\mathbf{W}} \mathcal{L}_{\text{DR}}^{\text{train}}((\boldsymbol{\alpha}; \mathbf{W}), D). \end{aligned} \quad (4)$$

*Differences from DARTS [93]:* Our DRC has essential differences from DARTS. *First*, we design an importance-aware search strategy to facilitate the channel number search for pruning. Instead, DARTS are designed for architecture design, which does not involve important channel selection. Therefore, it is easier for our proposed DRS than DARTS to identify the channel redundancy for each layer. Our searched model outperforms that searched by DARTS significantly (see results in Table IV). *Second*, the formulation of our dual regression-based channel number search (DRS) is different from DARTS. Our DRS is built upon our dual regression scheme, which helps to constrain the complex possible function space of the ill-posed SR optimization problem (see Theorem 1). Thus, our DRS

makes it easier to identify the layer-wise redundancy for channel pruning, resulting in lightweight SR models without significant performance degradation after channel pruning. Instead, without using the dual regression scheme, DARTS makes it hard to recognize the redundancy of SR models accurately. Thus, it may only obtain less compact models with larger performance degradation (see results in Table IV).

2) *Dual Regression Based Channel Pruning:* Based on the searched channel numbers, we still need to determine which channels should be pruned.

One of the key challenges is how to accurately evaluate the importance of channels.

To address this, we develop a dual regression channel pruning method that exploits the dual regression scheme to identify the important channels. We show our method in Fig. 3.

Let  $P$  and  $\widehat{P}$  be the original primal model and the compressed model, respectively. We use  $\mathbf{X}^{(l+1)}$  and  $\widehat{\mathbf{X}}^{(l+1)}$  to denote the output feature maps of the  $l$ th layer in  $P$  and  $\widehat{P}$ . Given the searched channel numbers  $\{\hat{c}_l\}_{l=1}^L$ , we seek to select the channels which really contribute to SR performance. Nevertheless, this goal is non-trivial to achieve due to the extremely large mapping space incurred by the ill-posed problem. To address this issue, we exploit the dual regression scheme to evaluate the importance of channels. Specifically, we consider one channel as an important one if it helps to reduce the dual regression loss  $\mathcal{L}_{\text{DR}}(\widehat{P}, D)$ . Moreover, for any layer  $l$ , we also minimize the reconstruction error [90], [102] of the feature maps between  $P$  and  $\widehat{P}$ , i.e.,  $\mathcal{L}_M(\mathbf{X}^{(l+1)}, \widehat{\mathbf{X}}^{(l+1)})$ , to further improve the performance. Given a specific channel number  $\hat{c}_l$ , we impose an  $\ell_0$ -norm constraint  $\|\mathbf{W}^{(l)}\|_0 \leq \hat{c}_l$  on the number of active channels in  $\mathbf{W}^{(l)}$ . Formally, the channel pruning problem for the  $l$ th layer is

$$\begin{aligned} & \min_{\mathbf{W}^{(l)}} \mathcal{L}_M(\mathbf{X}^{(l+1)}, \widehat{\mathbf{X}}^{(l+1)}) \\ & + \gamma \mathcal{L}_{\text{DR}}(\widehat{P}, D), \quad \text{s.t. } \|\mathbf{W}^{(l)}\|_0 \leq \hat{c}_l, \end{aligned} \quad (5)$$

where  $\gamma$  is a hyper-parameter that controls the weight of the dual regression loss (See more discussions on  $\gamma$  in Section V-E).

However, Problem (5) is hard to solve due to the training difficulty incurred by the  $\ell_0$ -norm constraint. To address this, we adopt a greedy strategy [60], [103], [104] in which we first remove all the channels and then select the most important channels one by one.

Following [60], we perform channel selection according to the gradients w.r.t. different channels.

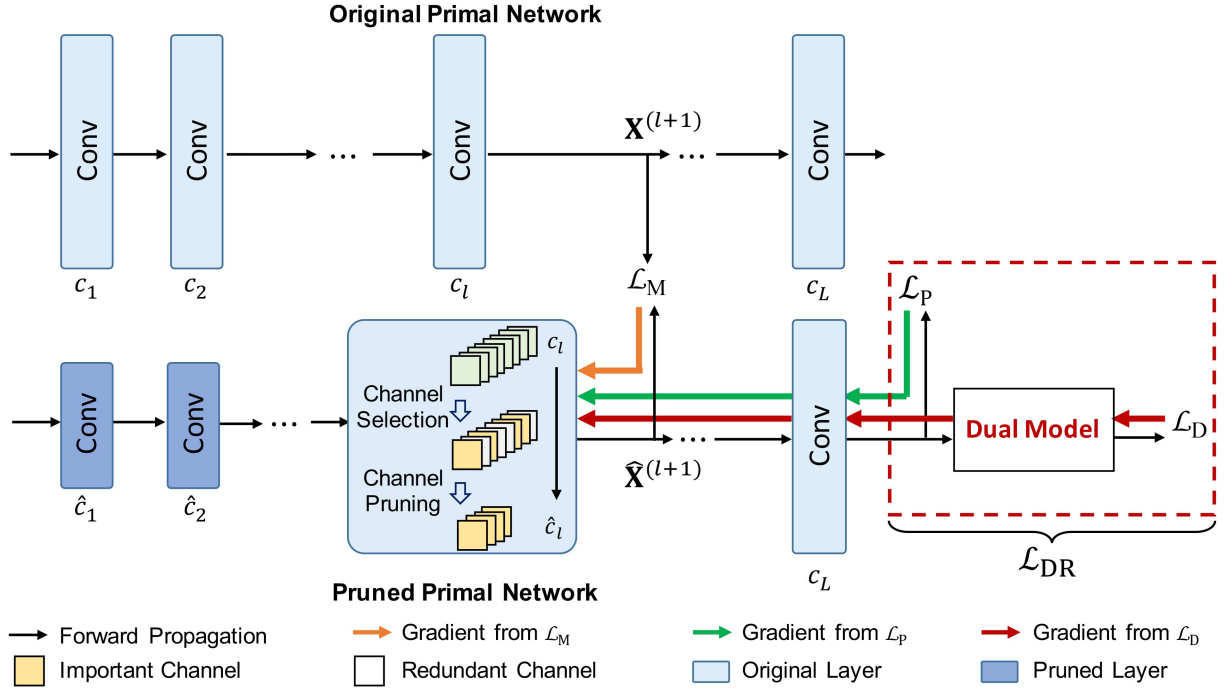


Fig. 3. The dual regression based channel pruning method. We evaluate the importance of channels by computing both the feature reconstruction loss  $\mathcal{L}_M$  and the dual regression loss  $\mathcal{L}_{DR}$ . Here,  $\mathbf{X}^{(l+1)}$  and  $\hat{\mathbf{X}}^{(l+1)}$  denote the output features of the  $l$ th layer in the original model and the pruned model, respectively.  $c_l$  and  $\hat{c}_l$  denote the channel number of the  $l$ th layer in the original model and the pruned model.

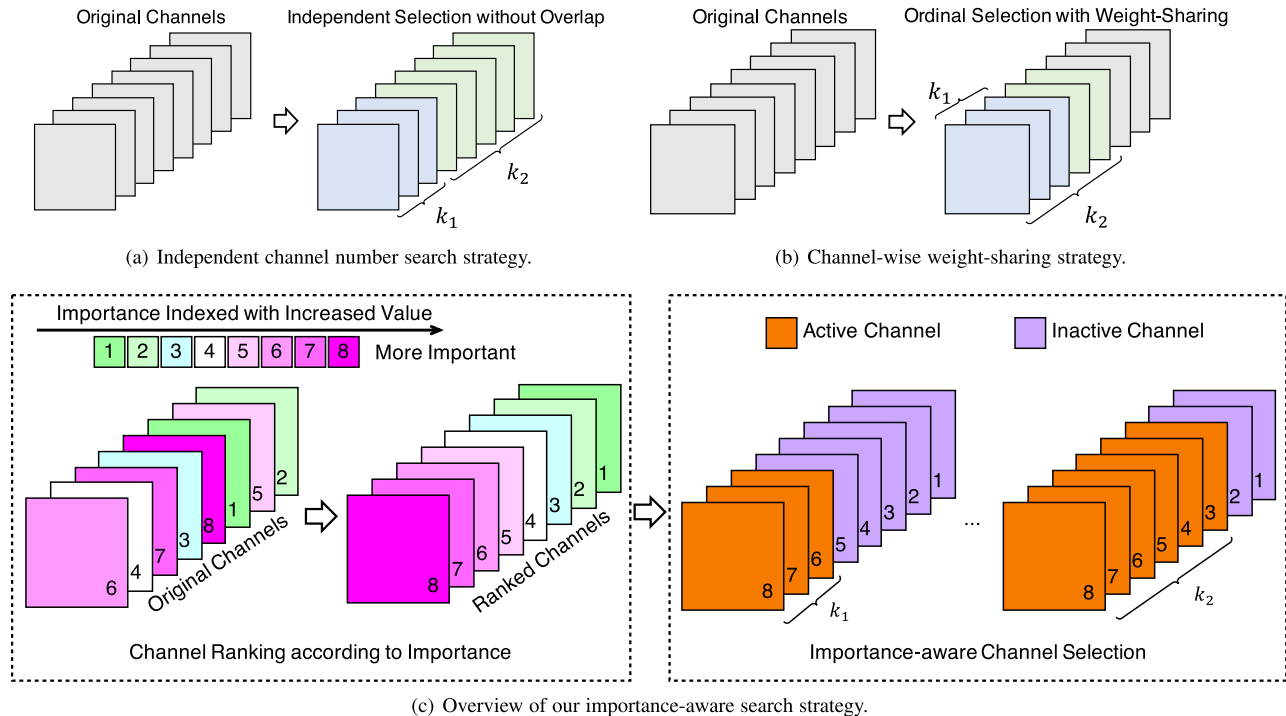


Fig. 4. Overview of most channel number search strategies and our importance-aware search strategy. (a) Some previous works [86], [87] assume that different channel configurations should be treated individually. For two candidate numbers of channels  $k_1$  and  $k_2$  ( $k_1 < k_2$ ), the selected  $k_2$  channels are independent of the  $k_1$  channels. (b) Some other works [65], [88], [89] use the weight-sharing strategy to reduce the search cost. For two candidate numbers of channels  $k_1$  and  $k_2$  ( $k_1 < k_2$ ), the selected  $k_2$  channels contain all the  $k_1$  channels. The weights of these overlapped channels are shared across different sets of channels during searching. (c) Based on the weight-sharing strategy, we further propose an importance-aware search strategy to search for a promising/suitable channel configuration to recognize and reduce layer-wise redundancy. For each candidate number of channels  $k$ , we select top- $k$  important channels and ignore the rest of the redundant channels simultaneously.

#### IV. EXPERIMENTS

We conduct extensive experiments to verify the effectiveness of the proposed methods. First, we evaluate the proposed dual regression (DR) learning scheme. Second, we compare the proposed dual regression compression (DRC) method with different model compression methods. Third, we further apply our DRC method to compress blind SR models. The source code is available at <https://github.com/guoyongcs/DRC>.

##### A. Datasets and Implementation Details

Based on the dual regression scheme, we build our DRN based on the design of U-Net for SR [105], [106] (See more details in the supplementary materials). We first propose two models, including a small model DRN-S and a large model DRN-L. We also apply our dual regression scheme to two popular SR models, i.e., SwinIR [44] and DAT [45]. Then, we use the proposed dual regression compression method to compress the DRN-S and SwinIR-light [44] models. By default, we consider the target pruning ratio of 30% in most experiments. We also conduct additional experiments with other pruning ratios  $r \in \{30\%, 50\%, 70\%\}$  and put the results in supplementary.

*Datasets and evaluation metrics:* Following [100], we train our models on DIV2K [107] and Flickr2K [17] datasets, which contain 800 and 2,650 images separately. For quantitative comparison, we evaluate different SR methods on five benchmark datasets, including Set5 [108], Set14 [109], BSDS100 [110], Urban100 [111] and Manga109 [112]. Moreover, for the blind SR setting where the degradation model of each test LR image is unknown, we use the DIV2KRK [113] dataset to evaluate the performance of different blind SR methods. To assess the quality of super-resolved images, we adopt two commonly used metrics, i.e., PSNR and SSIM [114]. The computational cost #MAdds are measured on a  $96 \times 96$  LR image.

*Training details:* During the training of our DRN-S and DRN-L, we apply Adam [115] with  $\beta_1 = 0.9$ ,  $\beta_2 = 0.99$  and set minibatch size as 32. We use RGB input patches with size  $48 \times 48$  from LR images and the corresponding HR patches as the training data, and augment the training data following the method in [17], [18]. The learning rate is initialized to  $10^{-4}$  and decreased to  $10^{-7}$  with a cosine annealing strategy. To train the SwinIR-DR and DAT-DR models, we follow the recipe of the training setting of SwinIR [44] and DAT [45], respectively. As for model compression, following the pruning pipeline of [60], [104], we take two lightweight models DRN-S and SwinIR-light [44] as the baselines, and conduct pruning followed by finetuning. For the blind SR setting, we randomly generate anisotropic Gaussian kernels to synthetic LR images from the given HR images following the setting in DCLS [116]. We use the synthetic LR-HR paired data to train and compress the baseline DCLS [116] model to obtain the lightweight DCLS-DRC model.

*Details of channel number search and channel pruning:* We search the channel numbers in each layer for the compressed models on DIV2K [107] dataset. We primarily consider removing  $r = 30\%$  to obtain more lightweight SR models for both our DRN-S and the SwinIR-light [44] models. Following [93],

we use zero initialization for the continuous variables  $\alpha$ , which ensures  $\alpha$  to receive sufficient learning signal at the early stage. We use Adam [115] optimizer to train the model with the learning rate  $\eta = 3 \times 10^{-4}$  and the momentum  $\beta = (0.9, 0.999)$ . We train the channel number search model for 100 epochs with a batch size of 16. The channel number search process takes approximately 10 hours on a TITAN A100 GPU. As for channel pruning, we perform dual regression channel pruning to select important channels on DIV2K [107] dataset. During pruning, once we remove the input channels of the  $l$ th convolution layer, the output channels of the previous convolution layer can be removed correspondingly. Once a new channel is selected, to reduce the performance drop, we apply the SGD optimizer with a learning rate of  $5 \times 10^{-5}$  to update the parameters of selected channels for one epoch.

##### B. Comparisons With State-of-the-Art SR Methods

In this experiment, we compare our method with state-of-the-art SR methods in terms of both quantitative results and visual results.

For the quantitative comparison, we show the PSNR and SSIM values of different methods for  $4\times$  super-resolution in Table I. For the quality comparison, we provide visual comparisons for our method and the considered methods in Fig. 5. We put more results in the supplementary materials.

From Table I, our proposed dual regression scheme is able to boost the training of the SR models. For example, the DAT-DR model equipped with our dual regression scheme achieves a better performance than the DAT [45] baseline. When compared with most state-of-the-art methods, our DAT-DR model consistently achieves the best performance on the five benchmark datasets. From Fig. 5, models equipped with our dual regression scheme, including our DRN-L, SwinIR-DR and DAT-DR, consistently produce sharper edges and shapes for both  $4\times$  SR. Instead, other baselines may produce blurrier ones (See more results in the supplementary materials). These results demonstrate the effectiveness of our dual regression scheme.

##### C. Comparisons With Lightweight SR Models

To demonstrate the effectiveness of our compression method, we compare our dual regression compression method and several representative channel pruning methods, including CP [121], Thinet [58], DCP [60] and SRP [73].

To this end, we apply the considered methods to compress our DRN-S model and the SwinIR-light [44] model for  $4\times$  SR. As shown in Table II, compared with the competitive lightweight models [53], [55], [70], [73], the model obtained by our DRC method is able to achieve better performance in terms of both PSNR and SSIM. Moreover, when comparing with different pruning strategies, our DRC is able to achieve lossless compression even when we consider very lightweight/compact models that are unlikely to have too much redundancy, e.g., SwinIR-light [44]. For example, the compressed SwinIR-light model (with 635 K parameters) obtained by our DRC scheme achieves similar performance to the baseline model (with 897 K parameters). Moreover, we provide visual comparisons for the

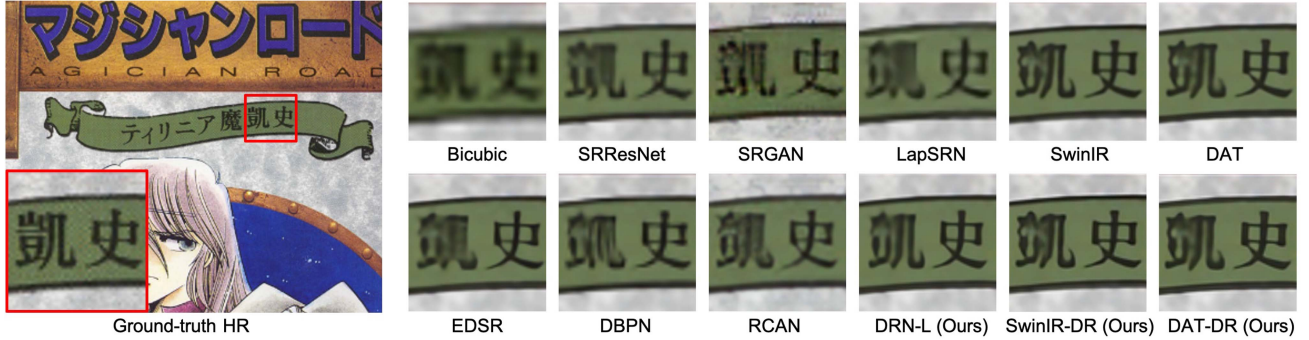


Fig. 5. Visual comparisons of the images produced by different models for  $4\times$  image super-resolution on benchmark datasets. We show that all the models enhanced by our DR consistently produce sharper images, i.e., with more high-frequency information, than their original counterparts.

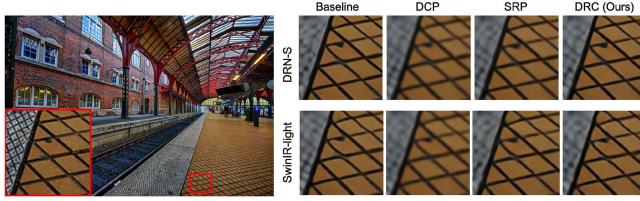


Fig. 6. Comparisons among different pruning methods based on both DRN-S and SwinIR-light. Our DRC consistently produces sharper images based on both DRN-S and SwinIR-light.

compressed SR models obtained by different compression methods in Fig. 6. Obviously, our DRC models consistently obtain promising SR images with clearer textures, showing the effectiveness of our proposed dual regression compression method.

#### D. Model Compression of Blind SR Models

In this part, we investigate the effect of our dual regression compression (DRC) scheme under the blind SR setting. We further apply our proposed compression scheme to the blind SR model DCLS [116] to obtain a more compact model named DCLS-DRC. We compare the compressed DCLS-DRC with existing state-of-the-art blind SR methods under the DIV2KRK [113] dataset. As shown in Table III, the compressed DCLS-DRC model even achieves a better performance than the baseline DCLS [116] model. Meanwhile, the DCLS-DRC model achieves the best performance on DIV2KRK [113] with less computational consumption than most existing blind SR methods. The results in Tables II and III demonstrate the effectiveness of our DRC under both the non-blind and the blind settings.

## V. FURTHER EXPERIMENTS

We provide more discussions on the proposed methods. First, we investigate the effect of the dual regression channel number search method in Section V-A. Second, we conduct ablation studies on the dual regression learning scheme in Section V-B. Third, we investigate the effect of the dual regression pruning method in Section V-C. Fourth, we analyze the effect of the hyper-parameter  $\lambda$  and  $\gamma$  in Sections V-D and V-E, respectively. Then, we analyze that the key component of our dual regression scheme in Sections V-F and V-G. Moreover, we further

TABLE V  
THE EFFECT OF THE PROPOSED DUAL REGRESSION LEARNING SCHEME ON SUPER-RESOLUTION PERFORMANCE IN TERMS OF PSNR SCORE ON THE FIVE BENCHMARK DATASETS FOR  $4\times$  SR

Model	Dual	Set5	Set14	BSDS100	Urban100	Manga109
DRN-S	✗	32.53	28.76	27.68	26.54	31.21
	✓	<b>32.68</b>	<b>28.93</b>	<b>27.78</b>	<b>26.84</b>	<b>31.52</b>
DRN-L	✗	32.61	28.84	27.72	26.77	31.39
	✓	<b>32.74</b>	<b>28.98</b>	<b>27.83</b>	<b>27.03</b>	<b>31.73</b>

TABLE VI  
THE EFFECT OF DUAL REGRESSION CHANNEL PRUNING ON THE MODEL COMPRESSION PERFORMANCE FOR  $4\times$  SR

Compression Ratio	Dual	Set5	Set14	BSDS100	Urban100	Manga109
30%	✗	32.53	28.73	27.60	26.67	31.25
	✓	<b>32.66</b>	<b>28.92</b>	<b>27.82</b>	<b>26.95</b>	<b>31.64</b>
50%	✗	32.38	28.67	27.53	26.47	31.09
	✓	<b>32.50</b>	<b>28.82</b>	<b>27.71</b>	<b>26.59</b>	<b>31.28</b>
70%	✗	32.31	28.65	27.63	26.35	30.88
	✓	<b>32.40</b>	<b>28.71</b>	<b>27.66</b>	<b>26.44</b>	<b>31.09</b>

investigate the effect of an additional cycle constraint on the HR domain in Section V-H.

#### A. Effect of Dual Regression Channel Number Search

We conduct an ablation study to verify the effect of our dual regression channel number search method. To be specific, we evaluate the baseline compression methods on our DRN-S model with a 30% compression ratio for  $4\times$  SR and show the experimental results in Table IV. Let “Manually Designed” denote the compression method that removes a specific number of channels in each layer (remove 30% channels in each layer). “Random Searched” denotes the compression method that randomly searches for a candidate scaling factor  $v$  to decide the channel numbers of each layer. As shown in Table IV, we find that weight sharing is able to greatly reduce the search cost while obtaining similar search results. More critically, when comparing the fifth and the sixth rows, the importance-aware search strategy is particularly effective in finding a smaller model but with better performance. If we further apply our dual regression scheme, we obtain the best result among the considered variants.

TABLE VII  
COMPARISON WITH THE BASELINE THAT USES DIFFERENT DUAL MODELS IN TERMS OF PSNR FOR  $4\times$  SR

Method	Set5	Set14	BSDS100	Urban100	Manga109
DRN-S without any dual model	32.53	28.76	27.68	26.54	31.21
DRN-S with a single dual model (without progressive)	32.63	28.87	27.73	26.71	31.40
DRN-S with more powerful dual models ( $2\times$ larger)	<b>32.69</b>	28.93	<b>27.80</b>	26.83	31.50
DRN-S (Ours)	32.68	<b>28.93</b>	27.78	<b>26.84</b>	<b>31.52</b>

We show that building the progressive dual models is able to improve the performance. Nevertheless, a small dual model is good enough compared to the  $2\times$  larger counterparts.

### B. Effect of Dual Regression Learning Scheme

We conduct an ablation study on our dual regression learning scheme and report the results for  $4\times$  SR in Table V. We evaluate the dual regression learning scheme on both our DRN-S and DRN-L models and show the experimental results on five benchmark datasets. From Table V, compared to the baselines, the models equipped with the dual regression learning scheme consistently yield better performance on all five benchmark datasets. These results suggest that our dual regression learning scheme improves the reconstruction of HR images by introducing an additional constraint to reduce the space of the mapping function. We also evaluate the effect of our dual regression learning scheme on other models, e.g., SRResNet [32] based network, which also yields similar results (See more results in the supplementary materials).

### C. Effect of Dual Regression Channel Pruning

In this part, we investigate the effect of the dual regression channel pruning method. Specifically, we evaluate our methods on our  $4\times$  DRN-S model with compression ratios of 30%, 50%, and 70%. From Table VI, with the dual regression channel pruning method, we are able to obtain lightweight SR models with better performance. Besides, the compressed models obtained by our dual regression channel pruning method consistently achieve higher SR performance on five benchmark datasets. This experiment demonstrates the effectiveness of our dual regression selection method to obtain efficient SR models.

### D. Effect of Hyper-Parameter $\lambda$ in (1)

We conduct an experiment to analyze the effect of the hyper-parameter  $\lambda$  in (1), which controls the weight of the dual regression loss. We analyze the effect of  $\lambda$  on the DRN-S and DRN-L models for  $4\times$  SR and compare the model performance on Set5. From Fig. 7(a), when we increase  $\lambda$  from 0.001 to 0.1, the dual regression loss gradually becomes more important and provides powerful supervision. If we further increase  $\lambda$  to 1 or 10, the dual regression loss term would overwhelm the original primal regression loss and hamper the final performance. To obtain a good tradeoff between the primal and dual regression, we set  $\lambda = 0.1$  in practice for the training of all DRN models.

### E. Effect of Hyper-Parameter $\gamma$ in (5)

We analyze the effect of the hyper-parameter  $\gamma$  in (5), which controls the weight of the dual regression loss on channel pruning. In particular, we investigate the effect of  $\gamma$  on the three compressed models for  $4\times$  SR and compared the model

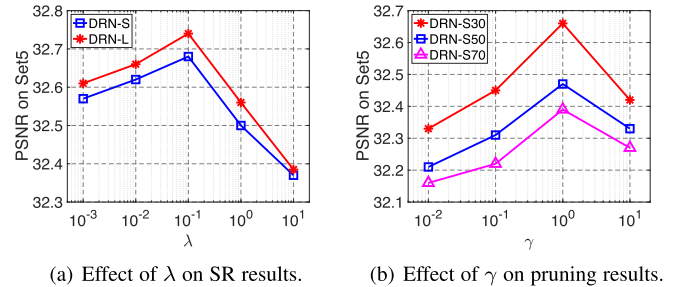


Fig. 7. Effect of the hyper-parameters  $\lambda$  and  $\gamma$  on the proposed dual regression learning and dual regression compression method.

performance on Set5. From Fig. 7(b), the compressed models perform best when  $\gamma$  is set to 1. If we increase or decrease the hyper-parameter  $\gamma$ , the compressed DRN models consistently yield worse SR performance on Set5. Therefore, we set  $\gamma = 1$  in practice to conduct the channel pruning on our DRN models.

### F. Effect of the Design of Dual Models

We compare our DRN with a new baseline method, which uses more powerful CNN networks as the dual model to provide the supervision signal from the low-resolution images. Experimental results in Table VII show that the simple dual models CNN networks are able to enhance SR performance. With more powerful dual models, the baseline model achieves similar improvement in performance. These results demonstrate that the closed form of our dual regression scheme is the key reason to boost the SR model training, instead of the design of the structure of dual models.

### G. Effect of the Progressive Dual Models

To investigate the effect of the progressive manner in our dual regression, we compare the baseline model that uses a single dual model that directly downsamples the images into the target resolution without the progressive scheme. As shown in Table VII, the baseline model without the progressive manner achieves a comparable performance. This model still achieves better performance compared with the baseline model without using the dual regression scheme. Moreover, we also investigate the effect of our dual regression scheme on transformer-based models, such as SwinIR [44] and DAT [45]. As shown in Table I, the models with a single dual model (i.e., DAT-DR) also achieve a significant improvement over the DAT [45] baseline model without the dual regression scheme. These results demonstrate

TABLE VIII  
THE EFFECT OF THE DUAL REGRESSION LOSS ON HR DATA FOR  $4 \times$  SR

Method	MAdds	Set5	Set14	BSDS100	Urban100	Manga109
DRN-S with dual HR	51.20G	32.69	28.93	27.79	26.85	31.54
DRN-S (Ours)	25.60G	32.68	28.93	27.78	26.84	31.52

DRN-S is taken as the baseline model.

that the closed-loop formulation of our dual regression scheme is the key factor for boosting the learning of SR models.

#### H. Effect of Dual Regression on HR Data

Actually, we can also add a constraint on the HR domain to reconstruct the original HR images. In this experiment, we investigate the effect of the dual regression loss on HR data and show the results in Table VIII. For convenience, we use “DRN-S with dual HR” to represent the model with the regression on both LR and HR images. From Table VIII, “DRN-S with dual HR” yields approximately  $2 \times$  training cost of the original training scheme but very limited performance improvement. Thus, we only apply the dual regression loss to LR data in practice.

## VI. CONCLUSION

In this paper, we have proposed a novel dual regression learning scheme to obtain effective SR models. Specifically, we introduce an additional constraint by reconstructing LR images to reduce the space of possible SR mapping functions. With the proposed learning scheme, we can significantly improve the performance of SR models. Based on the dual regression learning scheme, we further propose a lightweight dual regression compression method to obtain lightweight SR models. We first present a dual regression channel number search method to determine the redundancy of each layer. Based on the searched channel numbers, we then exploit the dual regression scheme to evaluate the importance of channels and prune those redundant ones. Extensive experiments demonstrate the superiority of our method over existing methods.

## REFERENCES

- [1] K. He, X. Zhang, S. Ren, and J. Sun, “Deep residual learning for image recognition,” in *Proc. IEEE Conf. Comput. Vis. Pattern Recognit.*, 2016, pp. 770–778.
- [2] O. Russakovsky et al., “ImageNet large scale visual recognition challenge,” *Int. J. Comput. Vis.*, vol. 115, no. 3, pp. 211–252, Dec. 2015.
- [3] Z. Wang, D. Liu, J. Yang, W. Han, and T. Huang, “Deep networks for image super-resolution with sparse prior,” in *Proc. IEEE Int. Conf. Comput. Vis.*, 2015, pp. 370–378.
- [4] W. Dong, P. Wang, W. Yin, G. Shi, F. Wu, and X. Lu, “Denoising prior driven deep neural network for image restoration,” *IEEE Trans. Pattern Anal. Mach. Intell.*, vol. 41, no. 10, pp. 2305–2318, Oct. 2019.
- [5] Y. Zhang, Y. Tian, Y. Kong, B. Zhong, and Y. Fu, “Residual dense network for image restoration,” *IEEE Trans. Pattern Anal. Mach. Intell.*, vol. 43, no. 7, pp. 2480–2495, Jul. 2021.
- [6] X. Deng and P. L. Dragotti, “Deep convolutional neural network for multi-modal image restoration and fusion,” *IEEE Trans. Pattern Anal. Mach. Intell.*, vol. 43, no. 10, pp. 3333–3348, Oct. 2021.
- [7] W.-S. Lai, J.-B. Huang, N. Ahuja, and M.-H. Yang, “Fast and accurate image super-resolution with deep Laplacian pyramid networks,” *IEEE Trans. Pattern Anal. Mach. Intell.*, vol. 41, no. 11, pp. 2599–2613, Nov. 2019.
- [8] W. Zhang, Y. Liu, C. Dong, and Y. Qiao, “RankSRGAN: Generative adversarial networks with ranker for image super-resolution,” in *Proc. IEEE Int. Conf. Comput. Vis.*, 2019, pp. 3096–3105.
- [9] X. Hu, H. Mu, X. Zhang, Z. Wang, T. Tan, and J. Sun, “Meta-SR: A magnification-arbitrary network for super-resolution,” in *Proc. IEEE Conf. Comput. Vis. Pattern Recognit.*, 2019, pp. 1575–1584.
- [10] S. Anwar and N. Barnes, “Densely residual Laplacian super-resolution,” *IEEE Trans. Pattern Anal. Mach. Intell.*, vol. 44, no. 3, pp. 1192–1204, Mar. 2022.
- [11] S. Zhou, J. Zhang, W. Zuo, and C. C. Loy, “Cross-scale internal graph neural network for image super-resolution,” in *Proc. Adv. Neural Inf. Process. Syst.*, H. Larochelle, M. Ranzato, R. Hadsell, M. Balcan, and H. Lin, Eds., 2020, pp. 3499–3509.
- [12] X. Kong, H. Zhao, Y. Qiao, and C. Dong, “ClassSR: A general framework to accelerate super-resolution networks by data characteristic,” in *Proc. IEEE Conf. Comput. Vis. Pattern Recognit.*, 2021, pp. 12011–12020.
- [13] J. Liang, K. Zhang, S. Gu, L. Van Gool, and R. Timofte, “Flow-based kernel prior with application to blind super-resolution,” in *Proc. IEEE Conf. Comput. Vis. Pattern Recognit.*, 2021, pp. 10596–10605.
- [14] J. Gu and C. Dong, “Interpreting super-resolution networks with local attribution maps,” in *Proc. IEEE Conf. Comput. Vis. Pattern Recognit.*, 2021, pp. 9195–9204.
- [15] D. Ulyanov, A. Vedaldi, and V. Lempitsky, “Deep image prior,” in *Proc. IEEE Conf. Comput. Vis. Pattern Recognit.*, 2018, pp. 9446–9454.
- [16] X. Wang, K. Yu, C. Dong, and C. C. Loy, “Recovering realistic texture in image super-resolution by deep spatial feature transform,” in *Proc. IEEE Conf. Comput. Vis. Pattern Recognit.*, 2018, pp. 606–615.
- [17] B. Lim, S. Son, H. Kim, S. Nah, and K. M. Lee, “Enhanced deep residual networks for single image super-resolution,” in *Proc. IEEE Conf. Comput. Vis. Pattern Recognit. Workshops*, 2017, pp. 136–144.
- [18] Y. Zhang, K. Li, K. Li, L. Wang, B. Zhong, and Y. Fu, “Image super-resolution using very deep residual channel attention networks,” in *Proc. Eur. Conf. Comput. Vis.*, 2018, pp. 286–301.
- [19] C. Dong, C. C. Loy, and X. Tang, “Accelerating the super-resolution convolutional neural network,” in *Proc. Eur. Conf. Comput. Vis.*, Springer, 2016, pp. 391–407.
- [20] Z. Hui, X. Wang, and X. Gao, “Fast and accurate single image super-resolution via information distillation network,” in *Proc. IEEE Conf. Comput. Vis. Pattern Recognit.*, 2018, pp. 723–731.
- [21] Y. Mei, Y. Fan, Y. Zhou, L. Huang, T. S. Huang, and H. Shi, “Image super-resolution with cross-scale non-local attention and exhaustive self-exemplars mining,” in *Proc. IEEE Conf. Comput. Vis. Pattern Recognit.*, 2020, pp. 5690–5699.
- [22] B. Niu et al., “Single image super-resolution via a holistic attention network,” in *Proc. Eur. Conf. Comput. Vis.*, 2020, pp. 191–207.
- [23] Y. Guo et al., “Closed-loop matters: Dual regression networks for single image super-resolution,” in *Proc. IEEE Conf. Comput. Vis. Pattern Recognit.*, 2020, pp. 5407–5416.
- [24] H. Hou and H. Andrews, “Cubic splines for image interpolation and digital filtering,” *IEEE Trans. Acoust., Speech, Signal Process.*, vol. 26, no. 6, pp. 508–517, Dec. 1978.
- [25] J. Allebach and P. W. Wong, “Edge-directed interpolation,” in *Proc. IEEE Int. Conf. Image Process.*, 1996, pp. 707–710.
- [26] X. Li and M. T. Orchard, “New edge-directed interpolation,” *IEEE Trans. Image Process.*, vol. 10, no. 10, pp. 1521–1527, Oct. 2001.
- [27] N. Nguyen and P. Milanfar, “An efficient wavelet-based algorithm for image superresolution,” in *Proc. IEEE Int. Conf. Image Process.*, 2000, pp. 351–354.
- [28] M. Haris, G. Shakhnarovich, and N. Ukita, “Deep back-projection networks for super-resolution,” in *Proc. IEEE Conf. Comput. Vis. Pattern Recognit.*, 2018, pp. 1664–1673.
- [29] Z. Li, J. Yang, Z. Liu, X. Yang, G. Jeon, and W. Wu, “Feedback network for image super-resolution,” in *Proc. IEEE Conf. Comput. Vis. Pattern Recognit.*, 2019, pp. 3867–3876.

- [30] A. Shocher, N. Cohen, and M. Irani, ““Zero-shot” super-resolution using deep internal learning,” in *Proc. IEEE Conf. Comput. Vis. Pattern Recognit.*, 2018, pp. 3118–3126.
- [31] J. Gu, H. Lu, W. Zuo, and C. Dong, “Blind super-resolution with iterative kernel correction,” in *Proc. IEEE Conf. Comput. Vis. Pattern Recognit.*, 2019, pp. 1604–1613.
- [32] C. Ledić et al., “Photo-realistic single image super-resolution using a generative adversarial network,” in *Proc. IEEE Conf. Comput. Vis. Pattern Recognit.*, 2017, pp. 4681–4690.
- [33] T. Tong, G. Li, X. Liu, and Q. Gao, “Image super-resolution using dense skip connections,” in *Proc. IEEE Int. Conf. Comput. Vis.*, 2017, pp. 4809–4817.
- [34] S. Baker and T. Kanade, “Limits on super-resolution and how to break them,” *IEEE Trans. Pattern Anal. Mach. Intell.*, vol. 24, no. 9, pp. 1167–1183, Sep. 2002.
- [35] M. Ben-Ezra, Z. Lin, and B. Wilburn, “Penrose pixels super-resolution in the detector layout domain,” in *Proc. IEEE Int. Conf. Comput. Vis.*, 2007, pp. 1–8.
- [36] Z. Lin and H.-Y. Shum, “Fundamental limits of reconstruction-based superresolution algorithms under local translation,” *IEEE Trans. Pattern Anal. Mach. Intell.*, vol. 26, no. 1, pp. 83–97, Jan. 2004.
- [37] C. Dong, C. C. Loy, K. He, and X. Tang, “Learning a deep convolutional network for image super-resolution,” in *Proc. Eur. Conf. Comput. Vis.*, Springer, 2014, pp. 184–199.
- [38] C. Dong, C. C. Loy, K. He, and X. Tang, “Image super-resolution using deep convolutional networks,” *IEEE Trans. Pattern Anal. Mach. Intell.*, vol. 38, no. 2, pp. 295–307, Feb. 2016.
- [39] J. Kim, J. Kwon Lee, and K. Mu Lee, “Accurate image super-resolution using very deep convolutional networks,” in *Proc. IEEE Conf. Comput. Vis. Pattern Recognit.*, 2016, pp. 1646–1654.
- [40] X. Mao, C. Shen, and Y.-B. Yang, “Image restoration using very deep convolutional encoder-decoder networks with symmetric skip connections,” in *Proc. Adv. Neural Inf. Process. Syst.*, 2016, pp. 2802–2810.
- [41] K. Zhang, W. Zuo, and L. Zhang, “Learning a single convolutional super-resolution network for multiple degradations,” in *Proc. IEEE Conf. Comput. Vis. Pattern Recognit.*, 2018, pp. 3262–3271.
- [42] Y. Zhang, Y. Tian, Y. Kong, B. Zhong, and Y. Fu, “Residual dense network for image super-resolution,” in *Proc. IEEE Conf. Comput. Vis. Pattern Recognit.*, 2018, pp. 2472–2481.
- [43] Y. Guo, Y. Luo, Z. He, J. Huang, and J. Chen, “Hierarchical neural architecture search for single image super-resolution,” *IEEE Signal Process. Lett.*, vol. 27, pp. 1255–1259, 2020.
- [44] J. Liang, J. Cao, G. Sun, K. Zhang, L. Van Gool, and R. Timofte, “SwinIR: Image restoration using swin transformer,” in *Proc. IEEE Int. Conf. Comput. Vis. Workshops*, 2021, pp. 1833–1844.
- [45] Z. Chen, Y. Zhang, J. Gu, L. Kong, X. Yang, and F. Yu, “Dual aggregation transformer for image super-resolution,” in *Proc. IEEE/CVF Int. Conf. Comput. Vis.*, 2023, pp. 12312–12321.
- [46] M. Zhang, Y. Fang, G. Ni, and T. Zeng, “Pixel screening based intermediate correction for blind deblurring,” in *Proc. IEEE/CVF Conf. Comput. Vis. Pattern Recognit.*, 2022, pp. 5892–5900.
- [47] Z. Wang, J. Chen, and S. C. Hoi, “Deep learning for image super-resolution: A survey,” *IEEE Trans. Pattern Anal. Mach. Intell.*, vol. 43, no. 10, pp. 3365–3387, Oct. 2021.
- [48] Y. Li et al., “NTIRE 2023 challenge on efficient super-resolution: Methods and results,” in *Proc. IEEE Conf. Comput. Vis. Pattern Recognit. Workshops*, 2023, pp. 1921–1959.
- [49] X. Zhang, H. Zeng, and L. Zhang, “Edge-oriented convolution block for real-time super resolution on mobile devices,” in *Proc. ACM Int. Conf. Multimedia*, 2021, pp. 4034–4043.
- [50] Q. Gao, Y. Zhao, G. Li, and T. Tong, “Image super-resolution using knowledge distillation,” in *Proc. Asian Conf. Comput. Vis.*, 2018, pp. 527–541.
- [51] W. Lee, J. Lee, D. Kim, and B. Ham, “Learning with privileged information for efficient image super-resolution,” in *Proc. Eur. Conf. Comput. Vis.*, 2020, pp. 465–482.
- [52] Y. Zhang, H. Chen, X. Chen, Y. Deng, C. Xu, and Y. Wang, “Data-free knowledge distillation for image super-resolution,” in *Proc. IEEE Conf. Comput. Vis. Pattern Recognit.*, 2021, pp. 7852–7861.
- [53] L. Wang et al., “Exploring sparsity in image super-resolution for efficient inference,” in *Proc. IEEE Conf. Comput. Vis. Pattern Recognit.*, 2021, pp. 4917–4926.
- [54] F. Yu, H. Li, S. Bian, and Y. Tang, “An efficient network design for face video super-resolution,” in *Proc. IEEE Int. Conf. Comput. Vis. Workshops*, 2021, pp. 1513–1520.
- [55] Z. Zhan et al., “Achieving on-mobile real-time super-resolution with neural architecture and pruning search,” in *Proc. IEEE Int. Conf. Comput. Vis.*, 2021, pp. 4821–4831.
- [56] S. Han, J. Pool, J. Tran, and W. Dally, “Learning both weights and connections for efficient neural network,” in *Proc. Adv. Neural Inf. Process. Syst.*, 2015, pp. 1135–1143.
- [57] S. Han, H. Mao, and W. J. Dally, “Deep compression: Compressing deep neural network with pruning, trained quantization and huffman coding,” in *Proc. Int. Conf. Learn. Representations*, 2016, pp. 1–14.
- [58] J. Luo, H. Zhang, H. Zhou, C. Xie, J. Wu, and W. Lin, “ThiNet: Pruning CNN filters for a thinner net,” *IEEE Trans. Pattern Anal. Mach. Intell.*, vol. 41, no. 10, pp. 2525–2538, Oct. 2019.
- [59] Y. Guo et al., “Towards accurate and compact architectures via neural architecture transformer,” *IEEE Trans. Pattern Anal. Mach. Intell.*, vol. 44, no. 10, pp. 6501–6516, Oct. 2022.
- [60] Z. Zhuangwei et al., “Discrimination-aware channel pruning for deep neural networks,” in *Proc. Adv. Neural Inf. Process. Syst.*, 2018, pp. 883–894.
- [61] M. Lin et al., “HRank: Filter pruning using high-rank feature map,” in *Proc. IEEE Conf. Comput. Vis. Pattern Recognit.*, 2020, pp. 1529–1538.
- [62] Z. Liu et al., “MetaPruning: Meta learning for automatic neural network channel pruning,” in *Proc. IEEE Conf. Comput. Vis. Pattern Recognit.*, 2019, pp. 3296–3305.
- [63] X. Dong and Y. Yang, “Network pruning via transformable architecture search,” in *Proc. Adv. Neural Inf. Process. Syst.*, 2019, pp. 759–770.
- [64] M. Lin, R. Ji, Y. Zhang, B. Zhang, Y. Wu, and Y. Tian, “Channel pruning via automatic structure search,” in *Proc. Int. Joint Conf. Artif. Intell.*, 2020, pp. 673–679.
- [65] J. Wang et al., “Revisiting parameter sharing for automatic neural channel number search,” in *Proc. 34th Int. Conf. Neural Inf. Process. Syst.*, 2020, pp. 5991–6002.
- [66] J. Frankle and M. Carbin, “The lottery ticket hypothesis: Finding sparse, trainable neural networks,” 2018, *arXiv: 1803.03635*.
- [67] Y. Guo, D. Stutz, and B. Schiele, “Improving robustness by enhancing weak subnets,” in *Proc. Eur. Conf. Comput. Vis.*, Springer, 2022, pp. 320–338.
- [68] V. Sehwag, S. Wang, P. Mittal, and S. Jana, “HYDRA: Pruning adversarially robust neural networks,” in *Proc. Adv. Neural Inf. Process. Syst.*, 2020, vol. 33, pp. 19655–19666.
- [69] B. Li et al., “Towards practical lottery ticket hypothesis for adversarial training,” 2020, *arXiv: 2003.05733*.
- [70] Z. Hou and S.-Y. Kung, “Efficient image super-resolution via channel discriminative deep neural network pruning,” in *Proc. IEEE Int. Conf. Acoust. Speech Signal Process.*, 2020, pp. 3647–3651.
- [71] C. R. Baker, “Joint measures and cross-covariance operators,” *Trans. Amer. Math. Soc.*, vol. 186, pp. 273–289, 1973.
- [72] Y. Li, S. Gu, K. Zhang, L. Van Gool, and R. Timofte, “DHP: Differentiable meta pruning via hypernetworks,” in *Proc. Eur. Conf. Comput. Vis.*, 2020, pp. 608–624.
- [73] Y. Zhang, H. Wang, C. Qin, and Y. Fu, “Learning efficient image super-resolution networks via structure-regularized pruning,” in *Proc. Int. Conf. Learn. Representations*, 2022, pp. 1–9. [Online]. Available: <https://openreview.net/forum?id=AjGC97Aofee>
- [74] J. Xin, N. Wang, X. Jiang, J. Li, H. Huang, and X. Gao, “Binarized neural network for single image super resolution,” in *Proc. Eur. Conf. Comput. Vis.*, 2020, pp. 91–107.
- [75] Y. Ma, H. Xiong, Z. Hu, and L. Ma, “Efficient super resolution using binarized neural network,” in *Proc. IEEE Conf. Comput. Vis. Pattern Recognit. Workshops*, 2019, pp. 694–703.
- [76] H. Li et al., “PAMS: Quantized super-resolution via parameterized max scale,” in *Proc. Eur. Conf. Comput. Vis.*, 2020, pp. 564–580.
- [77] D. He et al., “Dual learning for machine translation,” in *Proc. Adv. Neural Inf. Process. Syst.*, 2016, pp. 820–828.
- [78] Y. Xia, T. Qin, W. Chen, J. Bian, N. Yu, and T.-Y. Liu, “Dual supervised learning,” in *Proc. Int. Conf. Mach. Learn.*, 2017, pp. 3789–3798.
- [79] Y. Xia, X. Tan, F. Tian, T. Qin, N. Yu, and T.-Y. Liu, “Model-level dual learning,” in *Proc. Int. Conf. Mach. Learn.*, 2018, pp. 5383–5392.
- [80] Y. Zhang, T. Xiang, T. M. Hospedales, and H. Lu, “Deep mutual learning,” in *Proc. IEEE Conf. Comput. Vis. Pattern Recognit.*, 2018, pp. 4320–4328.

- [81] J.-Y. Zhu, T. Park, P. Isola, and A. A. Efros, "Unpaired image-to-image translation using cycle-consistent adversarial networks," in *Proc. IEEE Int. Conf. Comput. Vis.*, 2017, pp. 2223–2232.
- [82] Z. Yi, H. Zhang, P. Tan, and M. Gong, "DualGAN: Unsupervised dual learning for image-to-image translation," in *Proc. IEEE Int. Conf. Comput. Vis.*, 2017, pp. 2849–2857.
- [83] J. Cao, Y. Guo, Q. Wu, C. Shen, J. Huang, and M. Tan, "Adversarial learning with local coordinate coding," in *Proc. Int. Conf. Mach. Learn.*, 2018, pp. 707–715.
- [84] Y. Guo, Q. Chen, J. Chen, Q. Wu, Q. Shi, and M. Tan, "Auto-embedding generative adversarial networks for high resolution image synthesis," *IEEE Trans. Multimedia*, vol. 21, no. 11, pp. 2726–2737, Nov. 2019.
- [85] M. Mohri, A. Rostamizadeh, and A. Talwalkar, *Foundations of Machine Learning*. Cambridge, MA, USA: MIT Press, 2012.
- [86] J. Peng, M. Sun, Z.-X. Zhang, T. Tan, and J. Yan, "Efficient neural architecture transformation search in channel-level for object detection," in *Proc. Adv. Neural Inf. Process. Syst.*, 2019, pp. 14290–14299.
- [87] J. Fang, Y. Sun, Q. Zhang, Y. Li, W. Liu, and X. Wang, "Densely connected search space for more flexible neural architecture search," in *Proc. IEEE Conf. Comput. Vis. Pattern Recognit.*, 2020, pp. 10628–10637.
- [88] Z. Guo et al., "Single path one-shot neural architecture search with uniform sampling," in *Proc. 16th Eur. Conf. Comput. Vis.*, Glasgow, U.K., Springer, 2020, pp. 544–560.
- [89] A. Wan et al., "FBNNetV2: Differentiable neural architecture search for spatial and channel dimensions," in *Proc. IEEE Conf. Comput. Vis. Pattern Recognit.*, 2020, pp. 12965–12974.
- [90] H. Hao, A. Kadav, I. Durdanovic, H. Samet, and H. P. Graf, "Pruning filters for efficient ConvNets," in *Proc. Int. Conf. Learn. Representations*, 2017, pp. 1–13.
- [91] Y. He, G. Kang, X. Dong, Y. Fu, and Y. Yang, "Soft filter pruning for accelerating deep convolutional neural networks," in *Proc. Int. Joint Conf. Artif. Intell.*, 2018, pp. 2234–2240.
- [92] Y. He, J. Lin, Z. Liu, H. Wang, L.-J. Li, and S. Han, "AMC: Automl for model compression and acceleration on mobile devices," in *Proc. Eur. Conf. Comput. Vis.*, 2018, pp. 784–800.
- [93] H. Liu, K. Simonyan, and Y. Yang, "DARTS: Differentiable architecture search," in *Proc. Int. Conf. Learn. Representations*, 2019, pp. 1–13.
- [94] W. Shi et al., "Real-time single image and video super-resolution using an efficient sub-pixel convolutional neural network," in *Proc. IEEE Conf. Comput. Vis. Pattern Recognit.*, 2016, pp. 1874–1883.
- [95] W.-S. Lai, J.-B. Huang, N. Ahuja, and M.-H. Yang, "Deep Laplacian pyramid networks for fast and accurate super-resolution," in *Proc. IEEE Conf. Comput. Vis. Pattern Recognit.*, 2017, pp. 624–632.
- [96] Y. Tai, J. Yang, and X. Liu, "Image super-resolution via deep recursive residual network," in *Proc. IEEE Conf. Comput. Vis. Pattern Recognit.*, 2017, pp. 3147–3155.
- [97] N. Ahn, B. Kang, and K.-A. Sohn, "Fast, accurate, and lightweight super-resolution with cascading residual network," in *Proc. Eur. Conf. Comput. Vis.*, 2018, pp. 252–268.
- [98] Z. Hui, X. Gao, Y. Yang, and X. Wang, "Lightweight image super-resolution with information multi-distillation network," in *Proc. ACM Int. Conf. Multimedia*, 2019, pp. 2024–2032.
- [99] H. Zhao, X. Kong, J. He, Y. Qiao, and C. Dong, "Efficient image super-resolution using pixel attention," in *Proc. Eur. Conf. Comput. Vis. Workshops*, 2020, pp. 56–72.
- [100] X. Wang et al., "ESRGAN: Enhanced super-resolution generative adversarial networks," in *Proc. Eur. Conf. Comput. Vis. Workshops*, 2018, pp. 63–79.
- [101] T. Dai, J. Cai, Y. Zhang, S.-T. Xia, and L. Zhang, "Second-order attention network for single image super-resolution," in *Proc. IEEE Conf. Comput. Vis. Pattern Recognit.*, 2019, pp. 11065–11074.
- [102] J.-H. Luo, J. Wu, and W. Lin, "ThiNet: A filter level pruning method for deep neural network compression," in *Proc. IEEE Int. Conf. Comput. Vis.*, 2017, pp. 5058–5066.
- [103] S. Bahmani, B. Raj, and P. T. Boufounos, "Greedy sparsity-constrained optimization," *J. Mach. Learn. Res.*, vol. 14, pp. 807–841, 2013.
- [104] J. Liu et al., "Discrimination-aware network pruning for deep model compression," *IEEE Trans. Pattern Anal. Mach. Intell.*, vol. 44, no. 8, pp. 4035–4051, 2021.
- [105] Z. Iqbal, D. Nguyen, G. Hangel, S. Motyka, W. Bogner, and S. Jiang, "Super-resolution 1H magnetic resonance spectroscopic imaging utilizing deep learning," *Front. Oncol.*, vol. 9, pp. 1010–1021, 2019. [Online]. Available: <https://europepmc.org/articles/PMC6794570>
- [106] O. Ronneberger, P. Fischer, and T. Brox, "U-net: Convolutional networks for biomedical image segmentation," in *Proc. Int. Conf. Med. Image Comput. Comput.-Assist. Intervention*, 2015, pp. 234–241.
- [107] R. Timofte et al., "NTIRE 2017 challenge on single image super-resolution: Methods and results," in *Proc. IEEE Conf. Comput. Vis. Pattern Recognit. Workshops*, 2017, pp. 1110–1121.
- [108] M. Bevilacqua, A. Roumy, C. Guillemot, and M. Alberi-Morel, "Low-complexity single-image super-resolution based on nonnegative neighbor embedding," in *Proc. Brit. Mach. Vis. Conf.*, 2012, pp. 1–10.
- [109] R. Zeyde, M. Elad, and M. Protter, "On single image scale-up using sparse-representations," in *Proc. Int. Conf. Curves Surfaces*, Springer, 2010, pp. 711–730.
- [110] P. Arbelaez, M. Maire, C. Fowlkes, and J. Malik, "Contour detection and hierarchical image segmentation," *IEEE Trans. Pattern Anal. Mach. Intell.*, vol. 33, no. 5, pp. 898–916, May 2011.
- [111] J.-B. Huang, A. Singh, and N. Ahuja, "Single image super-resolution from transformed self-exemplars," in *Proc. IEEE Conf. Comput. Vis. Pattern Recognit.*, 2015, pp. 5197–5206.
- [112] Y. Matsui et al., "Sketch-based manga retrieval using Manga109 dataset," *Multimedia Tools Appl.*, vol. 76, no. 20, pp. 21811–21838, Oct. 2017.
- [113] S. Bell-Kligler, A. Shocher, and M. Irani, "Blind super-resolution kernel estimation using an internal-GAN," in *Proc. Adv. Neural Inf. Process. Syst.*, 2019, pp. 284–293.
- [114] Z. Wang, A. C. Bovik, H. R. Sheikh, and E. P. Simoncelli, "Image quality assessment: From error visibility to structural similarity," *IEEE Trans. Image Process.*, vol. 13, no. 4, pp. 600–612, Apr. 2004.
- [115] D. Kingma and J. Ba, "Adam: A method for stochastic optimization," in *Proc. Int. Conf. Learn. Representations*, 2015, pp. 1–15.
- [116] Z. Luo, H. Huang, L. Yu, Y. Li, H. Fan, and S. Liu, "Deep constrained least squares for blind image super-resolution," in *Proc. IEEE Conf. Comput. Vis. Pattern Recognit.*, 2022, pp. 17642–17652.
- [117] Y. Tai, J. Yang, X. Liu, and C. Xu, "MemNet: A persistent memory network for image restoration," in *Proc. IEEE Int. Conf. Comput. Vis.*, 2017, pp. 4539–4547.
- [118] W. Li, K. Zhou, L. Qi, N. Jiang, J. Lu, and J. Jia, "LAPAR: Linearly-assembled pixel-adaptive regression network for single image super-resolution and beyond," in *Proc. Adv. Neural Inf. Process. Syst.*, 2020, pp. 20343–20355.
- [119] X. Luo, Y. Xie, Y. Zhang, Y. Qu, C. Li, and Y. Fu, "LatticeNet: Towards lightweight image super-resolution with lattice block," in *Proc. 16th Eur. Conf. Comput. Vis.*, Glasgow, U.K., Springer, 2020, pp. 272–289.
- [120] X. Zhang, H. Zeng, S. Guo, and L. Zhang, "Efficient long-range attention network for image super-resolution," in *Proc. Eur. Conf. Comput. Vis.*, Springer, 2022, pp. 649–667.
- [121] Y. He, X. Zhang, and J. Sun, "Channel pruning for accelerating very deep neural networks," in *Proc. IEEE Int. Conf. Comput. Vis.*, 2017, pp. 1389–1397.
- [122] S. A. Hussein, T. Tirer, and R. Giryes, "Correction filter for single image super-resolution: Robustifying off-the-shelf deep super-resolvers," in *Proc. IEEE Conf. Comput. Vis. Pattern Recognit.*, 2020, pp. 1428–1437.
- [123] Y. Huang et al., "Unfolding the alternating optimization for blind super-resolution," in *Proc. 34th Int. Conf. Neural Inf. Process. Syst.*, 2020, pp. 5632–5643.
- [124] Z. Luo, Y. Huang, S. Li, L. Wang, and T. Tan, "End-to-end alternating optimization for blind super resolution," 2021, *arXiv:2105.06878*.
- [125] Y. Jo, S. W. Oh, P. Vajda, and S. J. Kim, "Tackling the ill-posedness of super-resolution through adaptive target generation," in *Proc. IEEE Conf. Comput. Vis. Pattern Recognit.*, 2021, pp. 16236–16245.
- [126] S. Y. Kim, H. Sim, and M. Kim, "KOALAnet: Blind super-resolution using kernel-oriented adaptive local adjustment," in *Proc. IEEE/CVF Conf. Comput. Vis. Pattern Recognit.*, 2021, pp. 10611–10620.
- [127] K. Zhang, L. V. Gool, and R. Timofte, "Deep unfolding network for image super-resolution," in *Proc. IEEE Conf. Comput. Vis. Pattern Recognit.*, 2020, pp. 3217–3226.
- [128] Z. Yue, Q. Zhao, J. Xie, L. Zhang, D. Meng, and K.-Y. K. Wong, "Blind image super-resolution with elaborate degradation modeling on noise and kernel," in *Proc. IEEE Conf. Comput. Vis. Pattern Recognit.*, 2022, pp. 2128–2138.
- [129] X. Kong, X. Liu, J. Gu, Y. Qiao, and C. Dong, "Reflash dropout in image super-resolution," in *Proc. IEEE Conf. Comput. Vis. Pattern Recognit.*, 2022, pp. 6002–6012.



**Yong Guo** received the bachelor's degree in software engineering from the South China University of Technology, in 2016, and the PhD degree from the South China University of Technology. He was a post-doctoral researcher with the Computer Vision and Machine Learning Group, Max Planck Institute for Informatics (MPI-INF). His research interests include deep learning and computer vision.



**Qi Chen** received the bachelor's degree in software engineering from the South China University of Technology, Guangzhou, China, in 2017, and the master's degree from the School of Software Engineering, South China University of Technology, in 2020. He is currently working toward the PhD degree with the Faculty of Engineering, Computer and Mathematical Sciences (ECMS), University of Adelaide. His research interests include deep learning and computer vision.



**Mingkui Tan** received the bachelor's degree in environmental science and engineering, in 2006, the master's degree in control science and engineering, in 2009, both from Hunan University in Changsha, China, and the PhD degree in computer science from Nanyang Technological University, Singapore, in 2014. He is currently a professor with the School of Software Engineering, South China University of Technology. From 2014–2016, he worked as a senior research associate on computer vision with the School of Computer Science, University of Adelaide, Australia. His research interests include machine learning, sparse analysis, deep learning and large-scale optimization.



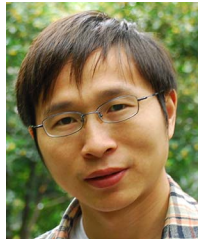
**Jiezhang Cao** received the BS degree in statistics from the Guangdong University of Technology, China, 2017, and the master's degree from the School of Software Engineering, South China University of Technology, China. He is currently working toward the PhD degree with the Department of Information Technology and Electrical Engineering, ETH Zürich. His current research interests include machine learning, and generative model.



**Zeshuai Deng** received the bachelor's degree in software engineering from the South China University of Technology, in 2019. He is currently working toward the PhD degree with the School of Software Engineering, South China University of Technology. His research interests include deep learning and computer vision.



**Yanwu Xu** received the BEng and PhD degrees from the University of Science and Technology of China, Hefei, China, in 2004 and 2009, respectively. He is the chief architect/scientist with the AI Innovation Business Department, Baidu Inc., Sunnyvale, California. He is also an adjunct professor with the Ningbo Institute of Materials Technology and Engineering, Chinese Academy of Sciences, Ningbo, China. His current research interests include ocular imaging, medical image analysis, computer vision, and machine learning. He has been an executive member of IEEE Engineering in Medicine and Biology Society and Intelligent Transportation Systems Society, Singapore Chapter, since 2014. He has been an associate editor of *BMC Medical Imaging* since 2015. He also served as an area chair for the International Conference on Medical Image Computing and Computer Assisted Intervention from 2017 to 2019.



**Jingdong Wang** received the BEng and MEng degrees from the Department of Automation, Tsinghua University, Beijing, China, in 2001 and 2004, respectively, and the PhD degree from the Department of Computer Science and Engineering, The Hong Kong University of Science and Technology, Hong Kong, in 2007. He is currently a senior researcher with the Visual Computing Group, Microsoft Research Asia. His areas of interest include deep learning, large-scale indexing, human understanding, and person re-identification. He is a fellow of IAPR. He is an associate editor of *IEEE Transactions on Multimedia* and *IEEE Transactions on Circuits and Systems for Video Technology*, and is an area chair (or SPC) of some prestigious conferences, such as CVPR, ICCV, ECCV, ACM MM, IJCAI, and AAAI.



**Jian Chen** received the BS and PhD degrees, both in computer science, from Sun Yat-sen University, Guangzhou, in 2000 and 2005 respectively. She is currently a professor with the School of Software Engineering (SSE), South China University of Technology, Guangzhou. She joined SSE with South China University of Technology as a faculty member, in 2005. Her research interests can be summarized as developing effective and efficient data analysis techniques for complex data and the related applications. Particularly, she is currently interested in various techniques of data mining, Web search, information retrieval, and recommendation techniques, as well as their applications.